MASTER'S THESIS

Master of Science in Advanced Mathematics and Mathematical Engineering

Title: Estimation of synaptic conductances using control theory

Author: Lluc Tresserras Pujadas

Advisor: Enric Fossas Colet and Antoni Guillamon Grabolosa

Department: Department of Systems Engineering, Automation, and Industrial Computing and Department of Mathematics

Academic year: 2019-2020

UNIVERSITAT POLITÈCNICA DE CATALUNYA
BARCELONATECH
Facultat de Matemàtiques i Estadística

I want to thank Dr. Enric Fossas Colet and Dr.Antoni Guillamon Grabolosa for supporting and helping me throughout the process of creation of this work. I also wanted to thank all my family, colleagues, and friends for encouraging and accompanying me throughout the work. I would like to give special thanks to my mother Montserrat, my father Rafel, my two brothers Jan and Cesc, and Marina, who have been by my side in recent years, advising me and giving me moral support at all times.

Abstract

Unveiling the input a neuron receives and distinguishing between excitation and inhibition provides information on local connectivity and brain operating conditions. However, experimental techniques do not allow direct recordings of synaptic inputs, and thus inverse methods are sought to retrieve synaptic currents/conductances from cell voltage. We propose a new method to estimate synaptic currents in neuron models using control theory (equivalent control and robust exact differentiation) and disentangle excitatory from inhibitory synaptic conductances.

Some irregularities make it impossible to deduce these conductances from the estimation of the synaptic current, therefore we introduce a second algorithm to estimate conductances inspired in an oversampling method presented by Bédard et al. that gives more successful results.

Contents

1. Introduction

Dynamical systems theory has always interested me, and these last years, one of my priorities has been studying its applications, which span to a wide variety of fields such as physics, engineering, chemistry, or economics. In this project, we will focus on the applications in biology, specifically in neuroscience.

Computational neuroscience is a branch of neuroscience that uses mathematical models to understand the principles that govern the development of the nervous system. The field of computational neuroscience began to be explored at the beginning of the last century.

Louis Lapicque was the first one to publish, in 1907, an article developing a model for a neuron, the integrate and fire model. However, a lot of people consider that the field of computational neuroscience started with the 1952 paper of Hodgkin and Huxley in which they describe, through nonlinear partial differential equations, the genesis of the action potential in the giant axon of the squid. The Hodgkin-Huxley equations have been the basis of the modern computational neuroscience and have inspired the development of new mathematics. The dynamical systems and computational methods are essential tools for the development of this field.

The main goal of these models is to understand the behavior of the neurons, and the interaction between them.

Neurons are cells that have the ability to communicate with each other through electrical or chemical signals. The information transmitted can amplify (excitation) or reduce (inhibition) the activity of the receiving neurons and so the activity of the brain. This exchange of information between neurons is called the synapse. The brain of an animal is formed by a large number of neurons (from thousands to billions). This increases the number of total connections between them (between 10^{14} and 10^{15}, for the human brain), so, increase the complexity of the brain.

A typical problem in computational neuroscience is the search of which signal is receiving a single neuron from the neurons it is connected to (synaptic signal), and then discern the temporal contributions of excitation from those of global inhibition.

A large number of synaptic contacts make unreachable to obtain directly the measurements of the synaptic currents that a neuron is receiving at each instant of time. A lot of methods have been developed in order to distinguish these two signals and despite of being based on different arguments, most of them have in common the use of inverse methods.

In this project, we will introduce a method to obtain the temporal contributions of global excitation and of global inhibition from experimental observation. So, we will be using an inverse method as a structure for the algorithm. Also, this method is based on control theory tools that we will present later.

In the Chapter 2, we will present an overview of how dynamical systems and computational analysis have been used in the construction of the main models that come out of neuroscience. This will give us the main idea of how a neuron works and the importance of understanding the role of the main variables and parameters on the behavior of the cell. We will focus on the construction of the Hodgkin-Huxley equations and the Morris-Lecar equations. These two models will be the basis of the method that we will present.

Chapter 3 is dedicated to the development of the control method for the synaptic term and the distinction of the excitatory and inhibitory signal from this synaptic current. We will explain the main arguments for the use of this method and the advantages and disadvantages that we have.

The algorithm used and the main results are presented in Chapter 4 we will be able to see that using the control method we obtain a good estimation of the synaptic term. However, some irregularities make it impossible to distinguish the excitatory and inhibitory signals. This forces us to introduce another method for the estimation of these signals even if the control theory is not going to be the basis of this alternative method.

We have to notice that this new method has not been developed with the precision that we have developed the control method because the main goal of this project was the use of the control method for the estimation of the excitatory and inhibitory signals.

For the development of this method, we have used C language to construct the necessary algorithms for the estimation of synaptic conductances. We can find the code in the next url: `https://web.mat.upc.edu/antoni.guillamon/Code/SynapticEstimationViaControl`.

2. Background

It is important to introduce background concepts about neuroscience and mathematics to deal with the problem that concerns us. This chapter will give us relevant information about the behavior of the brain, useful for the explanation, and construction of the main neuronal mathematical models.

We could write an entire work taking about all the concepts that we will introduce in this chapter because there is a large amount of information available talking about these topics, but we will only define and focus on the relevant concepts and necessary information to deal with the different models that we will use further and to understand the neurobiological problem under study.

We will start with the most important concept in brain science and the most basic structure in this field, the neuron. Our goal is to explain how a neuron works and the meaning of its behavior. Related to the neuron we have a lot of parameters and variables that influence the behavior of this type of cell. It is important to conjecture the meaning of these elements to have a general view of the neuron.

We also introduce the interaction between neurons, the synapse. We will explain how a neuron connects with other neurons of the network and how we can model this type of connection.

2.1 Important concepts about neurons

A human brain is formed by 10^{11} neurons, much fewer than the number of non-neuronal cells. But neurons are unique in the sense that they are the only cells that can transmit electrical signals over long distances.

A neuron typically has three parts: the soma, which contains the nucleus of the cell, the dendrites, the part of the neuron that receives the information that comes from other cells, and the axon, which is the part of the neuron that sends the information from the neuron to the others.

As every cell, a neuron has a membrane that distinguish the interior of the cell with the exterior. The utility of the membrane is to separate the concentration of ions of the two sides of it. This gives two different voltages: the voltage outside the cell, called V_{out}, and the voltage inside the cell, called V_{in}.

The study of a neuron is generally focused on the study of the potential due to charge separation across the cell membrane $V = V_{in} - V_{out}$, but by convention, it is taken $V_{out} = 0$. This potential is called the *membrane potential*, and most of existing models assume that it is homogeneous in all the soma.

A typical neuron receives inputs from more than 10 000 other neurons. The inputs produce electrical currents that change the membrane potential of the neuron, generally from the dendrites to the soma. Large electrical currents can lead to the generation of an *action potential* or *spike*, an abrupt and transient change of membrane voltage that propagates to other neurons via the axon. The spike is propagated along all the neurons of a network and it's the responsible of the information transmission between neurons. In general, neurons do not fire on their own, the generation of a spike is given by the result of incoming spikes from another neurons.

Now we have to introduce important concepts to understand the changes in the membrane potential that we could have during an action potential.

2.1.1 Resting potential

First of all, we introduce the *resting potential*, the potential across the membrane when the cell is at rest. A typical neuron has a resting potential of about $-70mV$.

The potential inside the cell will vary because of the exchange of ions between the interior and exterior of the neuron.

An inward current corresponds to a positively charged ion, such as Na^+, entering the cell. This inward current raises the membrane potential, the cell is *depolarized*. An outward current corresponds to a positively charged ion, such as K^+, leaving the cell. The membrane potential decreases and the cell becomes *hyperpolarized*. In the membrane of the cell there are channels that are responsible for these changes in the membrane potential, allowing the influx and outflux of ions that increase or decrease the membrane potential.

The principal ions that we can find on either side of the cell membrane are sodium (Na^+), potassium (K^+), chloride (Cl^-) and calcium (Ca^{2+}). Inside the cell, the concentration of K^+ is 10 times larger than outside. On the other hand, the concentration of Na^+ and Cl^- outside of the cell is larger than inside.

As we have said above, the exchange of ions between the inside and outside of the cell is possible thanks to channels contained in the membrane of the neuron, the most common ones being *ionic chanels* such that the Na^+, K^+, Cl^- and Ca^{2+} channels. We have two types of ionic channels in the membrane: the *leak channels* and the *voltage-gated channels*.

The voltage-gated channels are typically exclusive for a single ion. The membrane will be more permeable to the ions that have a larger number of open channels selective to them. Normally, the voltage-gated channels are closed when the cell is at rest. Those responsible for maintaining this state are the leak channels that are always open and make remain the neuron at the resting potential. So, the resting potential will be amplified by an incoming spike from other neurons, the voltage-gated channels will open and will lead to the generation of an action potential or spike.

The main goal of the cell is to maintain the charges inside and outside the neuron in equilibrium. During the action potential, when the membrane potential increases, some voltage-gated channels are open in order to decrease it.

The simplest theory of neuroscience describes the neurons as integrators with a threshold. A neuron may receive inputs from other neurons, called *postsynaptic potentials*, which modify the neuron's membrane potential. If the new value of the membrane potential holds below a given threshold, the neuron remains in the resting potential. If the postsynaptic potential is above the threshold, then the voltage-gated channels are open, an action potential occurs, and then resets its membrane potential.

2.1.2 Synapse

A synapse consists of an exchange of voltage between the pre-synaptic neuron and the post-synaptic neuron. The action potentials or spikes activate this transmission of information.

In the synapse, the action potential comes from the terminal part of the axon of the pre-synaptic neuron to the dendrite of the post-synaptic neuron. Except for electrical synapses the two implicated neurons are

not in touch, there is a space between the axon and the dendrites, also called *gap junctions*.

The last part of the axon of a pre-synaptic neuron contains small vesicles with different kinds of neurotransmitters inside such as Glutamate and GABA. When a synapse occurs, the vesicles are disintegrated and release the neurotransmitters at the free space which are eventually captured by the receptors of the dendrites that allow them to enter into the post-synaptic neuron. The entrance of these neurotransmitters can cause an increase, decrease of the membrane potential, or a non-response in the neuron.

2.2 Neuronal biophysics and modeling

In this chapter, we will formalize and mathematize the concepts introduced above. It's is important to understand and be familiarized with all these formalisms in order to construct the models used in this project. We will see that the neuron can be understood as a circuit in the electrical point of view, and we will explain how to model it. Also, we want to deal with the ionic channels and the ionic currents in order to model how the influx and outflux of ions vary the membrane potential.

2.2.1 Leak and ionic currents

The electric impulses of the neurons are generated and propagated via ionic currents. As we have said before, the concentration of these involved ions is different inside and outside of a cell, which creates electrochemical gradients. Outside the cell there is a larger concentration of Na^+ and Cl^-, and inside the cell we can find a higher concentration of K^+, and molecules with a negative charge (denoted as A^-). This concentration gradient, together with and electric potential gradient cause a constant exchange of ions between inside and outside of the neuron using the ionic channels.

For example, when the concentration of K^+ inside is higher than outside, then the leak channels allow the exit of the ions. While the ions are leaving, the cell carries a positive charge outside the neuron, and leaves a negative charge inside the cell. This two different charges accumulated on the opposite sides of the membrane surface create an electric potential gradient across the membrane. This electric potential reduces the outflux of K^+ caused by the attraction between K^+ and the interior of the cell that now has negative charge, and the repulsion from the positively charged exterior. We can see it in Figure 1.

When the concentration and electric gradient exert equal and opposite forces, they counterbalance each other and an equilibrium state is reached. This equilibrium is given by the Nernst equation:

$$V_{\mathrm{ion}} = \frac{RT}{zF} \ln \frac{[\mathrm{Ion}]_{\mathrm{out}}}{[\mathrm{Ion}]_{\mathrm{in}}}$$

where $[\mathrm{Ion}]_{\mathrm{in}}$ and $[\mathrm{Ion}]_{\mathrm{out}}$ are concentrations of the ions inside and outside the cell respectively. R is the universal gas constant with value $8,315 \frac{mJ}{(K^{\mathrm{o}} \cdot \mathrm{Mol})}$, T is temperature in degrees Kelvin, F is Faraday's constant, and z is the valence of the ion ($z = 1$ for K^+ and Na^+ and $z = -1$ for Cl^-).

We consider that V denotes the membrane potential and V_{Na}, V_{Ca} and V_{K} denote the Nerst equilibrium potentials or *reverse potentials*. Now using the definition of these concepts, we can define the net ion current that will describe the exchange of ions between the outside and inside of the cell membrane in terms of potential. We denote it as I_{ion}, and as it is clear that I_{ion} is equal to zero when $V = V_{\mathrm{ion}}$. In

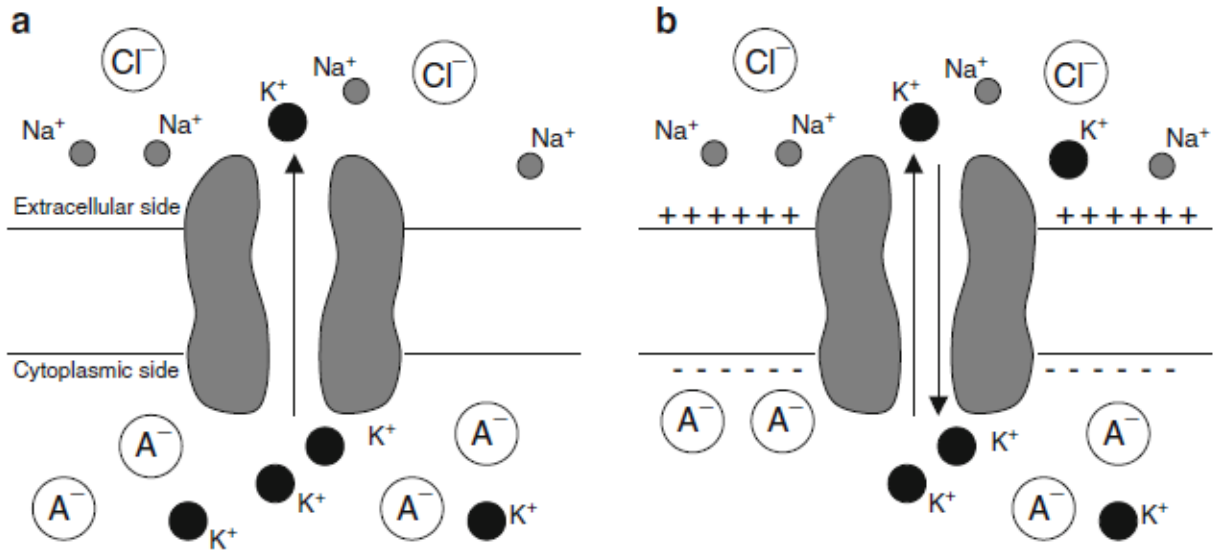

Figure 1: (a) In this figure we can see that the cell allows the outflux of K^+, and the concentration gradient of K^+ moves K^+ ions out of the cell. (b) The concentration of positive charge ions outside the cell increases, so, we have to reach an equilibrium when the electrical and chemical forces are equal and opposite. Image from [2].

general, the net ion current is proportional to the difference of potential:

$$I_{\text{ion}} = g_{\text{ion}}(V - V_{\text{ion}})$$

where g_{ion} is called ionic conductance with units (mS/cm^2).

In general, the conductances are not constant and depend on time. It is the time-dependent variation in conductances that allows a neuron to generate an action potential.

In the same way that we have introduced the ionic currents, we can introduce the *leak current*, $I_L = g_L(V - V_L)$ that controls the aperture of the leak channels. It corresponds to passive flow of ions through non-gated channels. Most of them control the inflow and outflow of K^+, so V_L will be close to V_K.

The leak conductance g_L, is constant. The conductances g_{Na} and g_K may change with time.

2.2.2 The analogy with an electric circuit.

To create the model of the neuron, first of all, we have to understand that we can represent the electric model of the neuron as an electrical circuit. This interpretation will give us a qualitative knowledge of the behavior of the membrane potential affected by the exchange of ions along the cell membrane.

A circuit consists of three components: The resistors, that will represent the ionic channels, the batteries, that will represent the concentration gradient of the ions, and the capacitors, representing the ability of the membrane to store charge.

The cell membrane is formed by a lipid bilayer and be interpreted as a capacitor. Using that, we can relate the charge stored and the potential in the following way:

$$q = CV$$

where q denotes the total charge, V is the potential, and the constant C is called the membrane capacitance. Notice that for larger neurons, we have larger total capacitance. Knowing that the current is the time

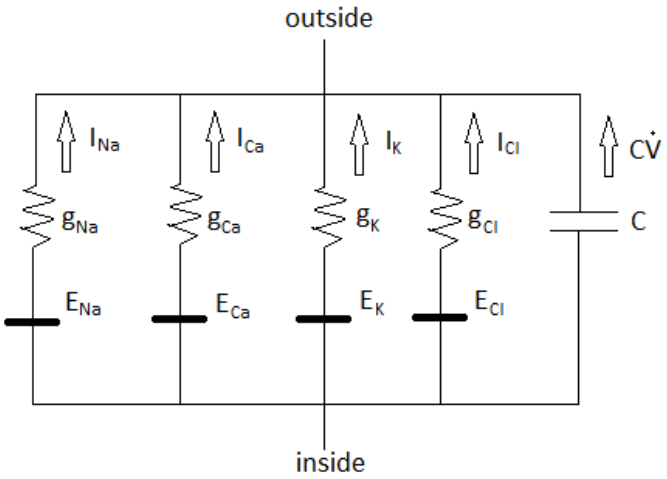

Figure 2: Representation of a neuron membrane as a circuit.

derivative of charge, differentiating the equation $q = CV$, we obtain the expression of the capacitance current:

$$i_{\text{cap}} = C\frac{dV}{dt}$$

We also have seen that the ionic current is:

$$I_{\text{ion}} = I_{\text{Na}} + I_{\text{K}} + I_{\text{Cl}}$$

Krichhoff's current law says that the total current into the cell must sum to zero. Adding to that the equivalent circuit representation, we obtain:

$$i_{\text{cap}} + I_{\text{ion}} = 0$$

$$C\frac{dV}{dt} = -I_{\text{ion}}$$

Assuming that we have a current source, called I_{app}, flowing into the cell membrane we have:

$$C\dot{V} = -I_{\text{Na}} - I_{\text{K}} - I_{\text{Cl}} + I_{\text{app}}$$

Notice that the membrane potential is typically bounded by the equilibrium potentials in the following way:

$$V_{\text{K}} < V_{\text{Cl}} < V < V_{\text{Na}} < V_{\text{Ca}}$$

So, we have that $I_{\mathrm{Na}}, I_{\mathrm{Ca}} < 0$. The negative sign of the currents means that are inward currents, and as $I_{\mathrm{K}}, I_{\mathrm{Cl}} > 0$, they are outward currents.

We have to notice that I_{Cl} is an outward current even though the flow of Cl^- ions is inward, but these ions are negatively charged, so it is equivalent to positively charged ions leaving the cell.

2.2.3 Resting potential

We have modeled the membrane potential as a differential equation, and we want to find for which value of the membrane potential the inward and outward currents balance each other. This value is called the *resting membrane potential*. If we only have K^+ channels and $I_{\mathrm{app}} = 0$, the membrane potential would tend to K^+ equilibrium potential which is around -90 mV.

$$0 = C\dot{V} = -g_{\mathrm{K}}(V - V_{\mathrm{K}})$$

$$V_{\mathrm{eq}} = V_{\mathrm{K}}$$

In the general case we have channels for each ion, so, we will have for example that the K^+ channels will produce a outward current of ions, so will decrease the membrane potential, but the Na^+ channels will allow the entrance of positive ions inside the cell. We have to find a equilibrium where the inflow and outflow of ions are balanced.

$$0 = C\dot{V} = -I_{\mathrm{Na}} - I_{\mathrm{K}} - I_{\mathrm{Cl}} + I_{\mathrm{app}}$$

$$V_{\mathrm{eq}} = \frac{g_{\mathrm{Cl}}V_{\mathrm{Cl}} + g_{\mathrm{Na}}V_{\mathrm{Na}} + g_{\mathrm{K}}V_{\mathrm{K}} + I_{\mathrm{app}}}{g_{\mathrm{Cl}} + g_{\mathrm{Na}} + g_{\mathrm{K}}}$$

If we consider that $I_{\mathrm{app}} = 0$ we have that:

$$V_{\mathrm{rest}} = \frac{g_{\mathrm{Cl}}V_{\mathrm{Cl}} + g_{\mathrm{Na}}V_{\mathrm{Na}} + g_{\mathrm{K}}V_{\mathrm{K}}}{g_{\mathrm{Cl}} + g_{\mathrm{Na}} + g_{\mathrm{K}}}$$

and we can write the circuit equation as:

$$C\dot{V} = I_{\mathrm{app}} - g_{\mathrm{ion}}(V - V_{\mathrm{rest}})$$

where g_{ion} is the total membrane conductance. We finally we can deduce that:

$$V \longrightarrow V_{\mathrm{rest}} + I_{\mathrm{app}}\frac{1}{g_{\mathrm{ion}}}$$

We have to notice that the total ionic conductance is dependent of V and time.

2.2.4 Ionic conductances

As we have said before, ionic channels let the inflow and outflow of the different ions. The conductances try to model the action of the *gates*, which switches the channels between open and closed states. These gates are sensitive to the membrane potential.

The ionic conductances can change along time, so we have to model them.

Knowing that, we rewrite the ionic currents as:

$$I_{\mathrm{ion}} = \bar{g_{\mathrm{ion}}}p_{\mathrm{ion}}(V - V_{\mathrm{ion}})$$

where p_{ion} is the average proportion of the ionic channels in the open state, that will depend on V and t, and $\bar{g_{\text{ion}}}$ is the maximal conductance of this ionic channels. Let's define more precisely p_{ion}.

There exist two types of gates. The gates that open the channels, and the gates that close them.

Hodgkin and Huxley studied the dynamics of K^+ and Na^+ conductances, and proposed a description of p_{ion}. This variable will depend on two different variables, m, and h.

- m denotes the probability of an activation gate being in the open state. Also can be denoted by the variable n. This variable is bounded by 0 and 1. We will consider $m = 0$ when the channel is deactivated and $m = 1$ when the channel is completely activated.
- h denotes the probability of an inactivation gate being in the open state. This variable also is bounded by 0 and 1, and we consider $h = 0$ when the channel is inactivated, and $h = 1$ when the channel is released from inactivation.

Using that, the proportion of open channels is:

$$p = m^a h^b$$

where a is the number of activation gates, and b is the number of inactivation gates per channel.

There exist some channels that do not inactivate so, we have persistent currents. In this case $b = 0$ and $p = m^a$. If we have channels that can be inactivated we have transient currents.

Let's describe the dynamics of the variables defined before. First of all we describe the dynamics of the activation variable m. As we have said before, we consider that the gates can be either open or closed. The probability that a gate is open or close will depend on the membrane potential. $\alpha_m(V)$ is the probability of a gate to go from closed to open state, and $\beta_m(V)$ is the probability of a gate to go from the open to closed state. If we consider that m is the fraction of open gates, then $1 - m$ is the fraction of closed gate, so:

$$\dot{m} = \alpha_m(V)(1 - m) - \beta_m(V)m = \frac{m_\infty(V) - m}{\tau_m(V)}$$

where:

$$m_\infty(V) = \frac{\alpha_m(V)}{\alpha_m(V) + \beta_m(V)} \text{ , and, } \tau_m(V) = \frac{1}{\alpha_m(V) + \beta_m(V)}$$

If V is constant, we have that the solution will be:

$$m(t) = m_\infty(V) + (m(0) - m_\infty(V))e^{-t/\tau_m(V)}$$

Using that, we can see that $m(t) \longrightarrow m_\infty(V)$.

The same can be done for the deactivation variable h. We will denote as $\alpha_h(V)$ the probability of a gate to go from open to closed state, and $\beta_h(V)$ the probability of a gate to go from closed to open state. h is the fraction of closed gates. We have:

$$\dot{h} = \alpha_h(V)(1 - h) - \beta_h(V)h = \frac{h_{\infty(V)} - h}{\tau_h(V)}$$

where:

$$h_\infty(V) = \frac{\alpha_h(V)}{\alpha_h(V) + \beta_h(V)} \text{ , and, } \tau_h(V) = \frac{1}{\alpha_h(V) + \beta_h(V)}$$

Hodgkin-Huxley proposed a expression for these expressions, $\alpha(V)$ and $\beta(V)$. The idea is that the probability of opening or closing a channel depends exponentially on the potential:

$$\alpha(V) = A_\alpha \exp(-B_\alpha V)$$

$$\beta(V) = A_\beta \exp(-B_\beta V)$$

2.3 Neuron models

In the previous chapter we have seen how we can model and understand the most important concepts in neurophisiology. We can use all these concepts to construct and develop the basic models of neuroscience. The main tool in the construction of these models is the dynamical systems theory, for analyzing nonlinear systems of differential equations. This theory allows as to study the geometric structure of phase space, and classify the types of solutions and extract some conclusions from that. In the case of the neuroscience, the dynamical systems can often predict if a model neuron will generate an action potential, if we will have oscillations, etc.

There are a lot of different neuroscience models, and each one is useful in different ways. Depending on your goal you will take a model or another. In this project we will focus on the Hodgkin-Huxley model, and the Morris-Lecar model.

2.3.1 Hodgkin-Huxley formalism

The Hodgkin-Huxley model is the most important in computational neuroscience. In 1952 Hodgkin and Huxley developed a theory that assumes that the squid axon carries three major currents: Voltage-gated persistent K^+ current with four activation gates, voltage-gated transient Na^+current with three activation gates and one inactivation gate, and the leak current, I_L, which allows the pass of Cl^- ions.

Knowing that we develop the following equations that will describe the model.

$$\begin{cases} C\dot{V} = -\bar{g_{Na}} m^3 h(V - V_{\mathrm{Na}}) - \bar{g_{\mathrm{K}}} n^4 (V - V_{\mathrm{K}}) - g_L(V - V_L) + I_{app} \\ \dot{m} = \phi(\frac{m_\infty(V) - m}{\tau_m(V)}) \\ \dot{h} = \phi(\frac{h_\infty(V) - h}{\tau_h(V)}) \\ \dot{n} = \phi(\frac{n_\infty - n}{\tau_n(V)}) \end{cases}$$

The parameter ϕ represents the temperature factor. The temperature at which an experiment is done can be determinant. The parameter ϕ appears when we model the channels gates because the channels are sensitive to the temperatures. Higher temperatures cause faster switching. The expression of this factor is the following one:

$$\phi = Q_{10}^{(T - T_{base})/10}$$

where T is the ambient temperature and Q_{10} is the ratio of the rates for an increase in temperature of 10°C. For the squid giant axon $T_{\mathrm{base}} = 6.3°C$ and $Q_{10} = 3$.

Also, Hodgkin and Huxley chose the following parameters and gating functions:

$$\bar{g_{\mathrm{Na}}} = 120\mathrm{mS/cm}^3 \ , \ \bar{g_{\mathrm{K}}} = 36\mathrm{mS/cm}^3 \ , \ g_L = 0.3\mathrm{mS/cm}^3$$

$$V_{\mathrm{Na}} = 50\mathrm{mV} \ , \ V_{\mathrm{K}} = -77\mathrm{mV} \ , \ V_L = -54.4\mathrm{mV}$$

The gate probabilities used are the following:

$$\alpha_n(V) = 0.01\frac{V+55}{1-\exp\left(\frac{-(V+55)}{10}\right)} \ , \ \beta_n(V) = 0.125\exp\left(\frac{-(V+65)}{80}\right)$$

$$\alpha_m(V) = 0.1\frac{V+40}{1-\exp\left(\frac{-(V+40)}{10}\right)} \ , \ \beta_m(V) = 4\exp\left(\frac{-(V+65)}{18}\right)$$

$$\alpha_h(V) = 0.07\exp\left(\frac{-(V+65)}{20}\right) \ , \ \beta_h(V) = \frac{1}{1+\exp\left(\frac{-(V+35)}{10}\right)}$$

If we plot the curves $n_\infty(V)$, $m_\infty(V)$ and $h_\infty(V)$ in Figure 3, we can see that n_∞ and m_∞ increase when

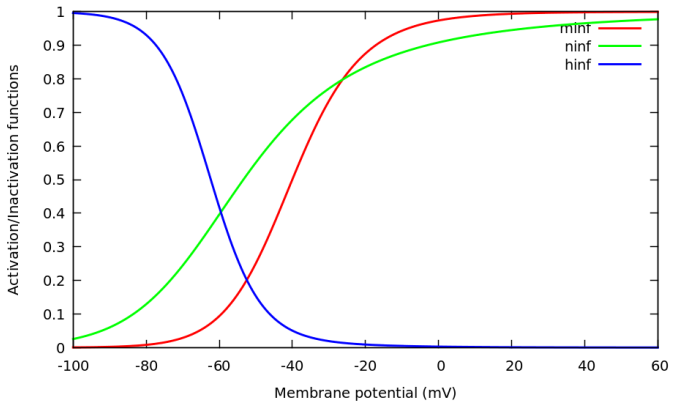

Figure 3: m_∞, n_∞ and h_∞ depending on V.

we increase the values of V. When we have a small value of V these functions approach to 0, and when we increase the value of V, the functions approach to 1. The function $h_\infty(V)$ is a decreasing function, and we can see that when the membrane potential is depolarized, $h_\infty \approx 0$. We can say that while we increase the membrane potential V, the K^+ channels open, whereas Na^+ channels both activate and inactivate.

In Figure 4 we can see the plots of τ_m, τ_h and τ_n. We can see that τ_m is much smaller than τ_h and τ_n, so, the Na^+ channels activate much faster than they inactivate or K^+ channels open. This follows that g_{Na} will increase faster than g_{K}.

Knowing this we can deduce the different changes in the membrane potential during an action potential. If the cell is at rest, if g_{Na} increases, then $I_K = g_{\mathrm{Na}}(V - V_{\mathrm{Na}})$ also will increase. The membrane potential V will increase because it will be dominated by Na^+ current until V approach to V_{Na}. When V arrive to this point, then, as we have seen before, the Na^+ channels inactivate, because at this point, $h \approx h_\infty(V) \approx 0$.

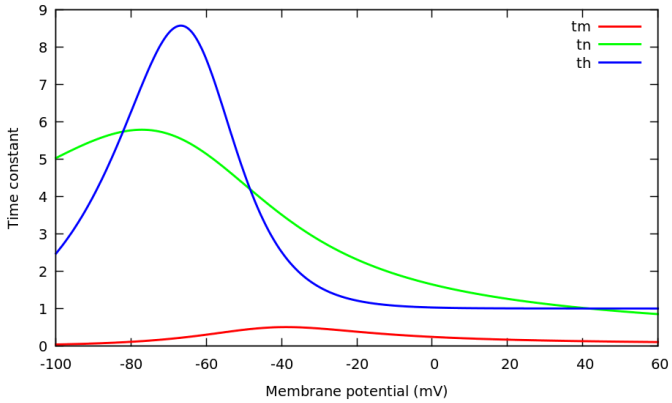

Figure 4: τ_m, τ_n, τ_h depending on V.

In the other hand, for this values of V, the K^+ channels open up, because $n \approx n_\infty(V) \approx 1$. The K^+ let the exit of positive ions, so the membrane potential will decrease until V approach to V_K.

After an action potential we reset the previous variables: $m_\infty = 0$, $n_\infty = 0$ and $h_\infty = 1$.

In this project, instead of working with the Hodgkin-Huxley equations, we will work with a simplicity of this model: The reduced Hodgkin-Huxley model.

The aim of this reduction is to transform the fourth dimensional Hodgkin-Huxley model into a two dimensional dynamical system. In the original Hodgkin-Huxely equations we have four variables (V, n, m, h) where V corresponds to the membrane potential and n, m, h are gatting variables. Now we introduce the two dimensional reduced Hodgkin-Huxley equations for (V, n).

$$\begin{cases} C\dot{V} = -\bar{g_{Na}} m^3 h(V - V_{\mathrm{Na}}) - \bar{g_\mathrm{K}} n^4 (V - V_\mathrm{K}) - g_L(V - V_L) + I_{app} \\ \dot{n} = \phi(\frac{n_\infty - n}{\tau_n(V)}) \end{cases}$$

The gating variables m and h are defined in the following way:

- In the original Hodgkin-Huxley equations we know that the dynamics of the gating variable m is the following:

  $$\dot{m} = \phi(\frac{m_\infty(V) - m}{\tau_m(V)})$$

  We can see that this equation has an invariant manifold $m(V) = m_\infty(V)$. Assuming that V_0 is the initial membrane potential, in the reduced Hodgkin-Huxley equations we will assume that $m(V_0) = m_\infty(V_0)$ so the trajectory of m will follow the trajectory of $m_\infty(V)$.

- To define the dynamics of h we will assume that h depends on n. It can be seen in Figure 3 and 4 that $h_\infty \approx 0.8 - n_\infty$ and τ_h and τ_n has similar behaviours. So, knowing that the gating variable h can be estimated knowing n in the following way:

  $$h(V) = 0.8 - n(V)$$

2.3.2 Morris-Lecar model

The Morris-Lecar equations are a reduced two-variable model. This model is considerably simpler than the Hodgkin-Huxley model but is able to exhibit the most important properties of the neuronal activity.

This model was proposed by Catherine Morris and Harold Lecar. It was developed to reproduce the variety of oscillatory behavior in relation to Ca^+ and K^+ conductance in the muscle fiber of the giant barnacle. They construct the model, assuming that the neuron has only three channels: A potassium channel, a leak channel and a calcium channel. We can simplify this model considering that the calcium conductance depends only on the voltage. Assuming that, we can construct the Morris-Lecar model in the following way:

$$\begin{cases} C\dot{V} = -\bar{g_{\mathrm{K}}} w(V - V_{\mathrm{K}}) - \bar{g_{Ca}} m_\infty(V)(V - V_{\mathrm{Ca}}) - g_L(V - V_L) + I_{app} \\ \dot{w} = \phi\left(\frac{w_\infty(V) - w}{\tau_w(V)}\right) \end{cases}$$

where

$$m_\infty(V) = \frac{1}{2}\left(1 + \frac{\tanh(V - V_1)}{V_2}\right)$$

$$w_\infty(V) = \frac{1}{2}\left(1 + \frac{\tanh(V - V_3)}{V_4}\right)$$

$$\tau_w(V) = \frac{1}{\cosh\left(\frac{V - V_3}{2V_4}\right)}$$

and V_1, V_2, V_3, V_4 are chosen parameters.

The interpretation of the dynamics of w is analog to the dynamics of the gating variables that appear in the Hodgkin-Huxley model explained in the previous chapter.

If we are interested in proving some properties of the neurons and in developing some theoretical results, the Morris-Lecar is a good model to start with because it's a simple and qualitative model. As

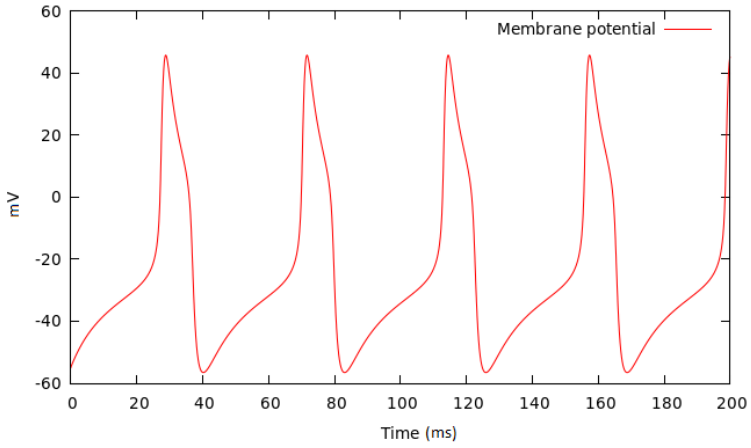

Figure 5: Solution of the Morris-Lecar system considering $Iapp = 45$.

we can see in Figure 5, the Morris-Lecar equations give a good approximation of the neuronal activity

and shows the main properties displayed by neurons. If we increase the value of I_{app}, the frequency of oscillations increase.

2.4 Synaptic Channels

Until now we have explained how to model a single neuron, the behavior of the neuron, and the different channels under the influence of an external potential I_{app}. If we want to construct a more realistic model of the neuronal activity we have to take into account that the neurons are in touch and they are connected.

We have seen that the membrane of the cell contains ionic and leak channels that allow the exchange of ions between the interior and the exterior of the neuron. There are many other channels on the membrane, and they are activated in different ways. In this chapter, we introduce the mechanism that allows the transmission of voltage between the different neurons of a network, the synapse.

The synapse involves two neurons: the pre-synaptic neuron, the neuron that transmits the information, and the post-synaptic neuron, which receives the voltage. The aperture of the synaptic channels and the transmission of the action potential between the pre-synaptic neuron and the post-synaptic neuron is given in the following way:

- The action potential of the pre-synaptic travels along the axon and arrives at the final part of the neuron called the synaptic terminal. There we have calcium channels that are activated by the action potential and release calcium.
- This calcium, at the same time, activates a calcium-binding protein that causes the release of neurotransmitters, which are in the interior of a vesicle, at the exterior of the cell, in the space between the two neurons called the synaptic cleft.
- The receptors on the dendrites of the post-synaptic cell receive the chemical signal of the transmitters and open some channels allowing the entrance of the neurotransmitters. These neurotransmitters can depolarize or hyperpolarize the neuron depending on their nature.

In order to add the synaptic term at the models defined in the previous chapter, we have to define some equations to model the synaptic current.

As for other currents, we model the synaptic currents as a product of conductance with a voltage difference:

$$I_{syn} = g_{syn}(t)(V - V_{syn})$$

where g_{syn} is the synaptic conductance, that depends on the pre-synaptic voltage, and V_{syn} is the synaptic reversal potential.

As we have said before, there a lot of different neurotransmitters, and when the post-synaptic neuron captures them, they can excite or inhibit the cell. To differentiate that in the formula of the synaptic current, we can express the previous expression is a sum of two parts: The excitatory current, and the inhibitory current.

$$I_{syn} = g_E(t)(V - V_E) + g_I(t)(V - V_I)$$

were g_E and V_E are the excitatory conductance and excitatory reversal potential respectively and g_I and V_I are the inhibitory conductance and inhibitory reversal potential respectively.

There are several ways to construct the conductance g_E, g_I, and g_{syn}. The modeling of this functions is not the principal aim of this project. We opt for a simple expression for the synaptic current because we are interested in the total excitatory and inhibitory conductances. To find more information about other constructions of the synpatic current look at [2].

The excitatory and inhibitory reversal potentials depend on the model that we are working on. In Hodgkin-Huxley equations we use $V_E = 0\mathrm{mV}$ and $V_I = -80\mathrm{mV}$. In Morris-Lecar equations we use $V_E = 10\mathrm{mV}$ and $V_I = -50\mathrm{mV}$.

To complete the model of the neuron that we have seen above, we have to add the synaptic current in order to model the connection of the cell with the neuronal network. For example, if we add the synaptic term in the Hodgkin-Huxley model we will finally have:

$$\begin{cases} C\dot{V} = I_{app} - \bar{g_{Na}} m^3 h(V - V_{\mathrm{Na}}) - \bar{g_{\mathrm{K}}} n^4 (V - V_{\mathrm{K}}) - g_L(V - V_L) - I_{syn} \\ \dot{m} = \phi(\frac{m_\infty(V) - m}{\tau_m(V)}) \\ \dot{h} = \phi(\frac{h_\infty(V) - h}{\tau_h(V)}) \\ \dot{n} = \phi(\frac{n_\infty - n}{\tau_n(V)}) \end{cases} \tag{1}$$

In the Morris-Lecar equations, the synaptic current $I_{syn} = g_E(t)(V - V_E) + g_I(t)(V - V_I)$ appears in the formula in the same way:

$$\begin{cases} C\dot{V} = -\bar{g_{\mathrm{K}}} w(V - V_{\mathrm{K}}) - \bar{g_{Ca}} m_\infty(V)(V - V_{\mathrm{Ca}}) - g_L(V - V_L) + I_{app} - I_{syn} \\ \dot{w} = \phi(\frac{w_\infty(V) - w}{\tau_w(V)}) \end{cases} \tag{2}$$

2.5 Sliding mode control

The main tool of the method presented at this project is the *sliding mode control*. Therefore, let's construct the fundamental background of theory of control to understand the construction of the method presented at the following chapter.

A plant (process) can be understood as a system with an input, and an output. A control system regulates the behavior of the process using control loops. In a control system we can identify the following elements: The *feedback controller* is the responsible of control the process. The control system compares the actual value of a *process variable* being controlled with the desired value or *setpoint*, and we use the difference as a control signal to modify the process to bring the process variable output to the setpoint.

There are two classes of control systems depending on the influence of the process variable on the behaviour of the system.

Systems in which the output quantity has no effect upon the input of the control process are called *open-loop control systems*. The control action from the controller is independent of the process variable. An example of open-loop system is a central heating boiler controlled only by a timer. The controller is the timer and the process variable is the building temperature.

The Close-loop Systems use the output of the system (or feedback signal) to both control and adjust the system. Therefore a closed-loop control system has the role of keeping a measured physical signal to the a predefined value (*setpoint*). An example of a closed-loop system is the same central heating boiler adding a thermostat. This system will give as feedback the actual temperature of the boiler and when the temperature reach the setpoint, the controller turns off. In Figure 6 we can see a diagram of a closed-loop system.

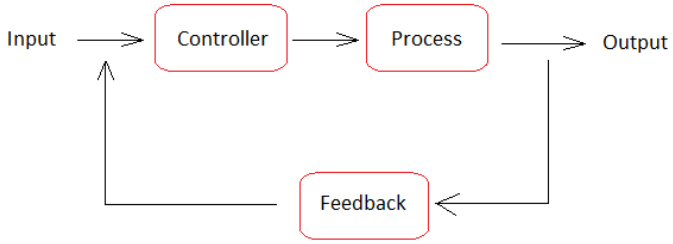

Figure 6: Diagram of a closed-loop system.

There are a lot of methods to control the behaviour of these variable. In this project we will have as process a non-linear differential equation, so, we will need a control method for non-linear differential equations. We will be using the sliding mode control.

The sliding mode control is a nonlinear control method that alters the dynamics of a nonlinear system by application of a discontinuous control signal (u) that forces the system to "slide" along a cross-section (*sliding surface*) of the system's normal behavior. Instead the control signal is not a continuous function of time, the system can switch from one continuous structure to another based on the current position in the state space. Let's explain a simlper idea of the sliding mode control.

Imagine that we want a ball to follow a desired trajectory (for example a straight). We get this kicking the ball in a transversal direction to the straight and against it. If the kicking frequency is infinite the ball will converge along the straight. See it in Figure 4.

Figure 7: Example of a sliding mode control.

The main idea of the sliding mode control is that given a nonlinear system, we add a control action to this system to make converge the trajectories to a given surface. Let's see it with an example.

Given the following linear system:

$$\begin{cases} \dot{x} = y \\ \dot{y} = k_1 x + k_2 y \end{cases} \tag{3}$$

depending on k_1 and k_2. Assume that $k_2 = 0.1$. We have that:

$$\begin{pmatrix} \dot{x} \\ \dot{y} \end{pmatrix} = M \begin{pmatrix} x \\ y \end{pmatrix}, \text{ where, } M = \begin{pmatrix} 0 & 1 \\ k_1 & 0.1 \end{pmatrix}$$

Let's compute the eigenvalues of the matrix M to understand the behavior of the system. Take two different values of k_1.

- If $k_1 = 1.5$, we have $\text{eig}(M) = \{1.2758, -1.1758\}$. This means that $p = (0, 0)$ will be a saddle point.
- If $k_1 = -1.5$, we have $\text{eig}(M) = \{0.05 + 1.22\text{i}, 0.05 - 1.22\text{i}\}$. This means that $p = (0, 0)$ will be a unstable focus.

See that in both cases, we have that $p = (0, 0)$ is an unstable equilibrium point.

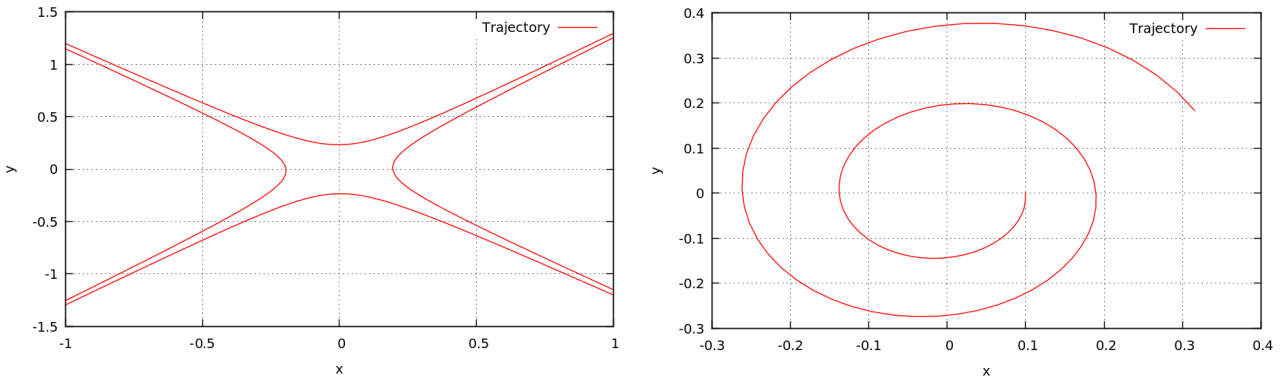

Figure 8: Phase space of the differential equation 3 taking $k_1 = -1.5$ (left figure) and $k_1 = 1.5$ (right figure).

The main propose of this example is the generation of a new differential equation combining the two previous equations and switching from one to the other using a control action. We want to create a new differential equation having $p = (0, 0)$ as a globally asymptotically stable equilibrium point.

We will assume that the following straight $r : y + x = 0$ is dividing our state space. Then, taking $s = y + x$, we will consider the following control action: $u = -k_1|x|sign(s)$. See that u will switch between $u = -k_1|x|$ and $u = k_1|x|$ depending on whether we are above or below the stright r.

Taking this expression for u, let's define the following differential equation taking $k_1 = 1.5$ and $k_2 = 0.1$:

$$\begin{cases} \dot{x} = y \\ \dot{y} = u + k_2 y \end{cases} \tag{4}$$

If we take an initial condition above the straight r, we have that $u = -k_1|x| < 0$. Knowing this we have that:

- If $x > 0$, the dynamic of y can be written as $\dot{y} = -k_1 x + k_2 y$, therefore, at this region (x, y) follows the dynamics of a focus.
- If $x < 0$, the dynamics of y can be written as $\dot{y} = k_1 x + k_2 y$, therefore, at this region (x, y) follows the dynamics of a saddle.

If we take an initial condition below the straight r, we have that $u = k_1|x| > 0$. Knowing this we have that:

- If $x < 0$, the dynamic of y can be written as $\dot{y} = -k_1 x + k_2 y$, therefore, at this region the dynamics (x, y) follows the dynamics of a focus.

- If $x > 0$, the dynamics of y can be written as $\dot{y} = k_1 x + k_2 y$, therefore, at this region (x, y) follows the dynamics of a saddle.

Using this, let's plot the dynamics of equation 4 in order to understand the previous arguments. We have computed them using a numerical integrator.

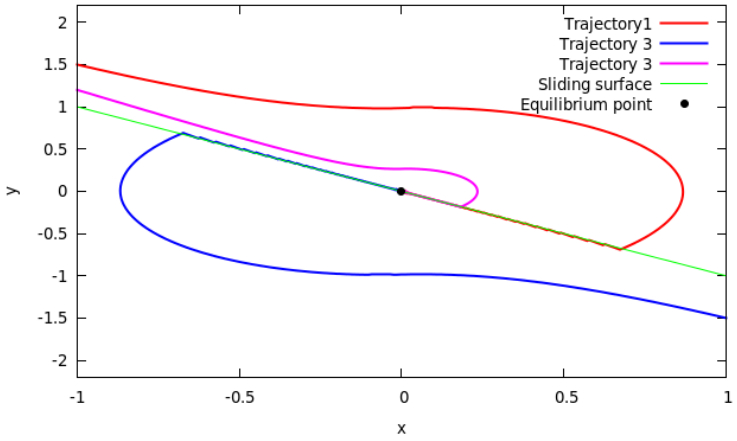

Figure 9: Phase space of the differential equation 4. See that all trajectories converge to $p = (0, 0)$, therefore this system has a globally asymptotically stable equilibrium point. Notice that the trajectories converge to p sliding along the straight $r : y + x = 0$.

Let's explain the convergence of every trajectory to the equilibrium point $p = (0, 0)$. The idea of the sliding mode control is to define a sliding surface $s(x, y) = 0$ and the variable $u(x, y)$ to get the convergence of the dynamics to the surface $s(x, y) = 0$. Therefore we need to define u such that given $(x, y) \in \mathbb{R}^2$:

- If $s(x, y) > 0$ the dynamic of (x, y) have to point to s. Therefore $\frac{ds}{dt} < 0$.
- If $s(x, y) < 0$ the dynamics of (x, y) have to point to s. Therefore $\frac{ds}{dt} > 0$.
- If $s(x, y) = 0$ the dynamics of (x, y) must to stay on the straight. Therefore $\frac{ds}{dt} = 0$.

Assuming that $s(x, y) = x + y$, $p = (0, 0)$ is a stable equilibrium point respect to the differential equation $\dot{s}(x, y) = 0$. Therefore, if all trajectories converge to $s(x, y) = 0$, the system will slide along the sliding surface toward this equilibrium. Notice that in the computational case a trajectory does not slide along the sliding surface. Instead of this the trajectory will oscillate around this straight r because u will be switching depending if we are above or below the straight.

In Figure 10 we can see how the variable u is switching the trajectory around the sliding surface r. In a general case, this constant switching, with high frequency around r, can lead to a failure. For this reason, in most of the sliding control methods we have an integrated *hysteresis* (*hys*).

The control variable u with hysteresis will not switch around the sliding surface but between an upper and a lower limit. This way, the frequency of the switching will decrease but the variation around the sliding surface will increase.

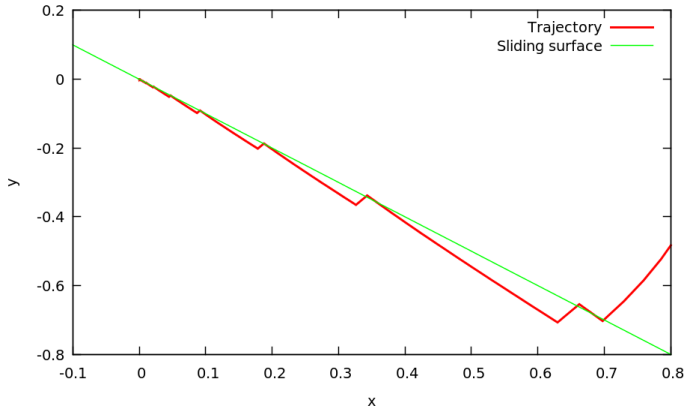

Figure 10: Oscillating behavior of the trajectory

Notice that if we take δ as integration step, and we assume that:

$$\delta, hys \to 0$$

we will not have the oscillation behavior of the trajectories any more. In this case the trajectory will slide along the sliding surface until p.

For more information about control theory and sliding mode methods see [5].

3. Control method for the synaptic parameter estimation

3.1 Introduction to the problem

In a neuronal network, the number of synaptic contacts is very large. There is a constant exchange of information between neurons and it is very difficult to obtain directly the synaptic currents that a neuron receives at every moment from an experiment. The extraction of the synaptic conductances from an experiment is a problem that has been extensively treated in the literature and many (partial) solutions have been suggested.

The general idea is to use an inverse method to estimate the synaptic conductances from experimental measures. From an experiment, it is relatively easy to extract the membrane potential at each moment of time from intracellular recordings of cortical cells. After getting it, we need a mathematical method in order to relate in some way the observed membrane potential to the synaptic conductances that we want to get.

Therefore, the use of this inverse method can provide some important errors in the estimation. In order to obtain effective solutions from it, we have to deal with some obstacles that can have a huge influence on the results.

The main problems that we can find are the choice of the model that we are going to use, the presence of noise in the observable data, the necessity of recording several membrane potential time courses and the inverse estimation problems that appear when we work with non-linear models. For each problem we can find in the literature a lot of articles with different methods to deal with them. Let us give a small explanation for every problem and see how this can affect the estimation of the synaptic conductances.

Assuming that we have a trajectory of the membrane potential as input, we have to notice that the extraction of data from an experimental observation is something delicate. The presence of noise into it can be determinant during the estimation. Some solutions have been developed for the treatment of the noise, both experimentally, and theoretically. Filtering the data before the use of a model is a typical strategy to treat the noise.

After solving this problem we need to fit the data into a mathematical model for a neuron in which the synaptic conductances are well identified. Most of the articles try to present a method as general as possible. The variety of neuron types makes it not highly recommended to use specific models because the membrane potential for these models will be very different for each type of neuron. It is more useful to use more qualitative methods that will provide the general behavior of a neuron.

Another important obstacle that all inverse methods, both experimentally and theoretically, have to take into account is the necessity of having to record a large number of membrane potential time courses assuming the invariance of the conductances for all recordings.

However, inverse methods provides excellent estimations in particular circumstances, special in subthreshold regimes, but we have problems when we try to use a linear models in the spiking regime. Most of the existent methods try to explain how to deal with these inverse estimations when the model is no longer

linear.

In the spiking regime, some nonlinear terms are active, and even filtering the membrane potential, the input-output relation is no longer linear. Also, this does not happen exclusively into the spiking zones since this nonlinear behaviour is present in the subthreshold regime due to the eventual activity of subthreshold ionic channels.

In this project, we present an inverse method for the estimation of the synaptic conductances based on the use of control theory techniques. Particularly, the method consists on using this techniques for the estimation of the synaptic current. This is something innovative in the sense that there are no previous works using this type of strategy for this problem.

The main idea is the creation of a variable $u(t)$ that we are going to control in order to approximate its values to the synaptic term I_{syn}, minimizing the errors as much as possible.

As we have said above, to develop the method that we want to present we have to deal with the possible obstacles.

We will see that using this method, the synaptic current I_{syn} can be estimated quite accurately, even in the spiking regimes. This means that we will not have problems to estimate the synaptic term in the non-linear zones. Also, we will see that to obtain a copy of the trajectory of I_{syn} we only need to record a single register of the membrane potential. However, we will see that the choice of the model that we are going to use is really important. The method is developed in such a way that can be adapted to any conductance-based models. Recall that the conductance-based models are the basic biophysical representation of an excitable cell, see Chapter 2.3.

We will see that our method works thanks to the gating variables having the following dynamics:

$$\dot{w} = \phi\left(\frac{w_\infty(V) - w}{\tau_w(V)}\right).$$

Therefore, our method will be extremely dependent on the model.

Let us introduce the main ideas of the method that we have developed and some of the theory behind the construction arguments.

3.2 Control theory method

The main idea of the method is the use of a sliding mode control with a control action u that, one filtered, will provide the trajectory of I_{syn}. After that, we can identify the excitatory and inhibitory conductances from I_{syn} by solving a system of equations.

As we have said above, we are talking about an inverse method whose goal is to estimate I_{syn} from experimental data of the membrane potential of a neuron. In this project we will develop this method using the Morris-Lecar equations and the reduced Hodgkin-Huxley model as connection between the observable data and the synaptic term. To avoid redundancies we will only construct the method using the Morris-Lecar equations. It is important to notice that this method is done once we have already registered the membrane potential from an experiment.

Suppose that this membrane potential $V(t)$ follows the following equations:

$$\begin{cases} C\dot{V} = I_{app} - \bar{g_{\mathrm{K}}} w(V - V_{\mathrm{K}}) - \bar{g_{Ca}} m_\infty(V)(V - V_{\mathrm{Ca}}) - g_L(V - V_L) - I_{syn} \\ \dot{w} = \phi(\frac{w_\infty(V) - w}{\tau_w(V)}) \end{cases}$$

We will create a copy of the Morris-Lecar model with an extra input term u instead of the synaptic input I_{syn}. With this change we will have to define two new variables $\hat{V}$ and $\hat{w}$ instead of V and w in the following way:

$$\begin{cases} C\dot{\hat{V}} = I_{app} - \bar{g}_{\mathrm{K}} \hat{w}(V - V_{\mathrm{K}}) - \bar{g}_{Ca} m_\infty(V)(V - V_{\mathrm{Ca}}) - g_L(V - V_L) - u \\ \dot{\hat{w}} = \phi(\frac{w_\infty(V) - \hat{w}}{\tau_w(V)}) \end{cases} \tag{5}$$

Notice that we are using the known variable V that we have obtained from experimental measurements for the construction of the new model that describes the dynamics of $\hat{V}$ and $\hat{w}$.

Our objective is to obtain the trajectory of the variable $u(t)$ so that $u \simeq I_{syn}$. At first, we can not assure that $u = I_{syn}$, so, we have to introduce these two new variables $\hat{V}$ and $\hat{w}$ to describe the new model. Let us see how we can work with these variables in order to reach our goal.

We define two new variables: $e_V = V - \hat{V}$ and $e_w = w - \hat{w}$. If we design $u(t)$ so that

$$e_V, e_w \longrightarrow 0, \tag{6}$$

then we can conclude that for $\varepsilon << 1$, $\exists t_V > 0$ such that $\forall t > t_V \ |V(t) - \hat{V}(t)| < \epsilon$, and $\exists t_w > 0$ such that $\forall t > t_w \ |w(t) - \hat{w}(t)| < \epsilon_w$. If we see (6), then it is clear that $u \simeq I_{syn}$.

To see whether e_V and e_w converge to zero, we can construct the dynamics of e_V and e_w and work from these two equations:

$$\begin{cases} C\dot{e_V} = -\bar{g_{\mathrm{K}}} e_w(V - V_{\mathrm{K}}) + I_{syn} - u \\ \dot{e_w} = -\phi \frac{1}{\tau_w(V)} e_w \end{cases}$$

Also, we will try to do the same assuming that the membrane potential $V(t)$ follows the reduced Hodgkin-Huxley model.

As we have done with the Morris-Lecar equations, we will make a copy of the reduced Hodgkin-Huxley model:

$$\begin{cases} C\dot{\hat{V}} = I_{app} - \bar{g_{Na}} m^3 h(V - V_{\mathrm{Na}}) - \bar{g_{\mathrm{K}}} \hat{n}^4(V - V_{\mathrm{K}}) - g_L(V - V_L) - u \\ \dot{\hat{n}} = \phi(\frac{n_\infty - \hat{n}}{\tau_n(V)}) \end{cases} \tag{7}$$

So, after this introduction, the main goal of the project will be the definition of the variable u so that (6) is fulfilled.

We will define the variable $u(t)$ for the Morris-Lecar equations. The construction of $u(t)$ using the reduced Hodgkin-Huxley equations will be analogous to the $u(t)$ of the Morris-Lecar construction, so we will not focus on it.

First of all let's see if e_w converges to zero for every expression of u.

3.2.1 Convergence of e_w

As we have said before, the trajectory of e_w will depend on the observable data of the membrane potential V and time t:

$$\frac{de_w}{dt} = -f(V)e_w$$

where $f(V) = \phi\frac{1}{\tau_w(V)}$.

Let us study the behavior of $f(V)$. Remember that

$$\tau_w(V) = \frac{1}{\cosh\left(\frac{V-V_3}{2V_4}\right)}$$

defines a probability, so $\tau_w(V) \in [0,1]$, $\forall V$. In Figure 11 we can see the graph of this function.

Since $\phi > 0$ is a positive parameter different from 0, it is clear that $f(V)$ will be a positive-definite function, $f(V) > 0$, for any value of V.

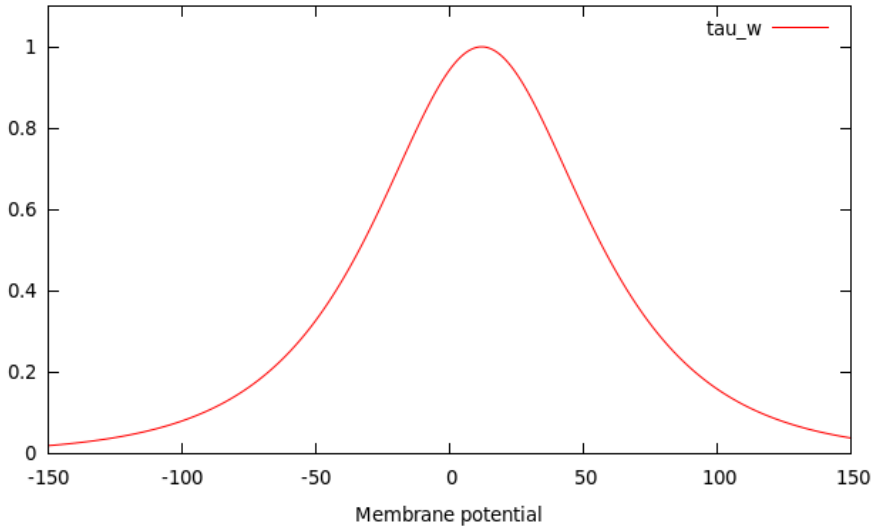

Figure 11: Graphic of τ_w with $V_3 = 12$ and $V_4 = 17.4$.

Now, let us study the dynamics of e_w. First of all, we need to introduce some definitions that will be useful to study the dynamics of the variable e_w.

Definition 3.1. A *Lyapunov function* for an autonomous dynamical system

$$\begin{cases} g : \mathbb{R}^n \longrightarrow \mathbb{R}^n \\ \dot{y} = g(y) \end{cases}$$

with an equilibrium point at $y = 0$ is a scalar function $L : \mathbb{R}^n \longrightarrow \mathbb{R}$ that is continuous, has continuous first derivatives, is locally positive-definite, and the time derivative of the Lyapunov function is locally positive-definite.

We want to define a Lyapunov function for the dynamics of e_w.

We can see that in our case, we have an autonomous dynamical system with $g(e_w) = -f(V)e_w$. Let us find if we have equilibrium points:

$$\frac{de_w}{dt} = 0 \iff -\phi\frac{1}{\tau_w(V)}e_w = 0$$

Since $f(V) > 0$, for whatever value of V, we have:

$$-f(V)e_w = 0 \iff e_w^{eq} = 0$$

So, there is only one equilibrium point, $e_w^{eq} = 0$. Let us study the stability of $e_w^{eq} = 0$.

We define a new scalar function L in the following way:

$$\begin{aligned} L : \mathbb{R} &\longrightarrow \mathbb{R} \\ e_w &\mapsto e_w^2 \end{aligned}$$

Let us see if this function L is a Lyapunov function. It is easy to prove that it is continuous and its derivative $L'(e_w) = 2e_w$ is also continuous. Also it is a positive-definite function.

Let us compute the time derivative of the Lyapunov function:

$$\frac{dL}{dt} = \frac{dL}{de_w}\frac{de_w}{dt} = 2e_w \cdot (-f(V)e_w),$$

and let us see if it is locally positive-definite:

$$\frac{dL}{dt} = -2f(V)e_w^2.$$

We know that both $f(V)$ and e_w^2 are positive-definite, so $\frac{dL}{dt}$ will be negative-definite.

We conclude that $L(e_w) = e_w^2$ is a Lyapunov function for the dynamics of e_w. Knowing that, we introduce a new theorem.

Theorem 3.2. *If the Lyapunov-candidate function L is globally positive-definite, radially unbounded, the equilibrium isolated and the time derivative of the Lyapunov-candidate function is globally negative-definite:*

$$\dot{L}(x) < 0 \ , \ \forall x \in \mathbb{R}^n \backslash \{0\},$$

then the equilibrium is globally asymptotically stable.

In our case, we have already seen that the Lyapunov function is globally positive-definite. Also, it is radially unbounded since:

$$\lim_{e_w \to \infty} L(e_w) = \infty$$

We can see that $e_w = 0$ is isolated because is the unique equilibrium point of the system. Previously we have seen that the time derivative of the Lyapunov function is globally negative-definite.

Under these assumptions we finally can conclude that $e_w \to 0$.

This shows us what we were looking for:

$$\lim_{t\to\infty} e_w(t) = 0.$$

That is, the error for w will converge to zero.

Notice that for the reduced Hodgkin-Huxley equations, e_n have similar behavior as e_w: $e_n = 0$ is the unique equilibrium point, and $L(e_n) = e_n^2$ is a Lyapunov function for the reduced Hodgkin-Huxley model and the equilibrium point.

Therefore, also the error for n will converge to zero.

3.2.2 Convergence of e_V

The dynamic of e_V is the following:

$$C\dot{e_V} = -\bar{g_{\mathrm{K}}} e_w (V - V_{\mathrm{K}}) + I_{syn} - u$$

We will use a *sliding mode control* to define u in order to force e_V converge to zero.

The sliding mode control will be used to maintain the trajectory of e_V near to zero along time to converge to zero in finite time. For this purpose, we are going to define a new function $U(t)$ such that:

$$U(t) \geq |-g_{\mathrm{K}}(V(t) - V_{\mathrm{K}})e_w(t) + I_{syn}(t)|.$$

Using this last definition we will introduce the function u as:

$$u(t) = U(t) \cdot \mathrm{sign}(e_V(t))$$

Let us see how this control works at instant t^*:

- If $e_V(t^*) > 0$, we want to decrease e_V in order to force e_V converge to zero.
  We need $\dot{e_V}(t^*) < 0$, and so, we need to define $u(t^*)$ such that:
  $$-\bar{g_{\mathrm{K}}} e_w(t^*)(V(t^*) - V_{\mathrm{K}}) + I_{syn}(t^*) - u(t^*) < 0,$$
  or, equivalently,
  $$u(t^*) > -\bar{g_{\mathrm{K}}} e_w(t^*)(V(t^*) - V_{\mathrm{K}}) + I_{syn}(t^*).$$
  Therefore, $u(t^*) = U(t^*) = U(t^*) \cdot \mathrm{sign}(e_V(t^*))$.
- If $e_V(t^*) < 0$ we want to increase e_V in order to force e_V converge to zero
  We need to $\dot{e_V}(t^*) > 0$, so, we need to define $u(t^*)$ so that:
  $$-\bar{g_{\mathrm{K}}} e_w(t^*)(V(t^*) - V_{\mathrm{K}}) + I_{syn}(t^*) - u(t^*) > 0$$
  or, equivalently,
  $$u(t^*) < -\bar{g_{\mathrm{K}}} e_w(t^*)(V(t^*) - V_{\mathrm{K}}) + I_{syn}(t^*)$$
  Therefore, $u(t^*) = -U(t^*) = U(t^*) \cdot \mathrm{sign}(e_V(t^*))$

Using this sliding mode control, we maintain e_V oscillating around 0. The control action $u = U \cdot \text{sign}(e_V)$ forces e_V converge to zero in finite time.

3.2.3 Estimation of I_{syn}

Let us try to give a more specific definition of the function U.

We have seen that $\lim_{t\to\infty} e_w(t) = 0$, so, it is clear that

$$\lim_{t\to\infty} U(t) \geq \lim_{t\to\infty} |-g_{\text{K}}(V(t) - V_{\text{K}})e_w(t) + I_{syn}(t)| = |I_{syn}(t)| \tag{8}$$

Assuming that $I_{syn}(t)$ is a bounded function,8 has an absolute minimum m_{syn} and an absolute maximum M_{syn}.

We can define U as $U(t) = \max\{|M_{syn}|, |m_{syn}|\}$. Then u is going to oscillate between U and $-U$ in order to control the trajectory of e_V. In Figure 12 we can see the oscillating behaviour of u.

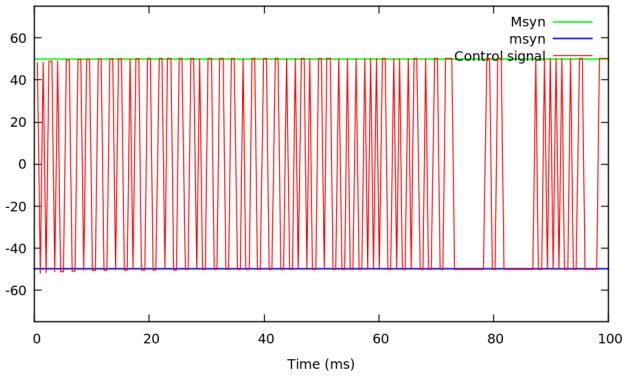

Figure 12: Plot of the trajectory $u(t)$.

Filtering the input $u(t)$ we obtain an estimation of I_{syn}. To filter the control action $u(t)$ we define a *filtration variable* y following the differential equation filter

$$\begin{cases} \tau_y \dot{y} = -(y - u) \\ u(t) = U(t) \cdot \text{sign}(t) \end{cases}$$

The filtration variable y will be an approximation of the synaptic term I_{syn}.

3.2.4 Estimation of the synaptic conductances

Remember that the expression of the synaptic current is

$$I_{syn}(t) = g_E(t)(V(t) - V_E) + g_I(t)(V(t) - V_I) \tag{9}$$

where $V(t)$, V_E and V_E are assumed to be known. Applying the methodology explained in the previous chapters, we are also able to approximate the time course of I_{syn}.

From this information, we would like to distinguish the synaptic conductances $g_E(t)$ and $g_I(t)$. It's clear

that we don't have enough information to determine the two conductances, from the synaptic current, at every instant of time. Let' see that.

We assume that, as input, we have a discretization of the trajectory of V. We have defined V for a set of instant of time $\{t_0, t_1, ..., t_n, ..., t_N\}$. We have the same for the trajectory of I_{syn}.

Therefore, to distinguish the synaptic conductances from 9 we make the following "oversampling" approximation: we suppose that g_E and g_I can be represented with half the sampling frequency as that of I_{syn}, which corresponds to the time series of $N/2$ values.

This means that assuming the previous discretitzation of the membrane potential, we impose that $\forall n \in [0, \frac{N-1}{2}] \cap \mathbb{N}$:

$$g_{E\,2n} = g_{E\,2n+1}$$

$$g_{I\,2n} = g_{I\,2n+1}$$

where $g_{E\,n} = g_E(t_n)$ and $g_{I\,n} = g_I(t_n)$.

Using that, $\forall n \in [0, \frac{N-1}{2}] \cap \mathbb{N}$ we can construct the following system of equations:

$$\begin{cases} I_{syn_{2n}} = g_{E\,2n}(V_{2n} - V_E) + g_{I\,2n}(V_{2n} - V_I) \\ I_{syn_{2n+1}} = g_{E\,2n}(V_{2n+1} - V_E) + g_{I\,2n}(V_{2n+1} - V_I) \end{cases}$$

Solving it, we will get the trajectories of the synaptic conductances g_E and g_I.

This idea for the distinction of the synaptic conductances from the estimated synaptic current is similar to a method presented by Bédard et al., see [1]. The authors propose a method for the extraction of the excitatory and inhibitory conductances from a single-trial membrane potential recordings, based on oversampling the membrane potential.

4. Algorithm and numerical results

In the previous chapter, we have explained the main idea of the method that we have used and the theoretical background that support it. In this chapter, we will explain the main steps of a numerical algorithm that develops the method from above. At the same time, we will show some of the results that we have obtained using this algorithm.

We have seen that this conductance estimation method is an inverse method that uses experimental observable data only. Even if it is typical to have observable data of the membrane potential of a neuron as input, in our algorithm, we use a generated data of the synaptic conductances g_E and g_I. Specifically a file with values of g_E and g_I at every 0.01 milliseconds. We have taken this synaptic conductances from a computational model because in the absence of experimental conductances the optimal move is to choose them from a realistic neuronal network. In this case we have taken them that a neuron from hte McLaughlin network receive over one second (see it [4]). Let's plot the synaptic conductances:

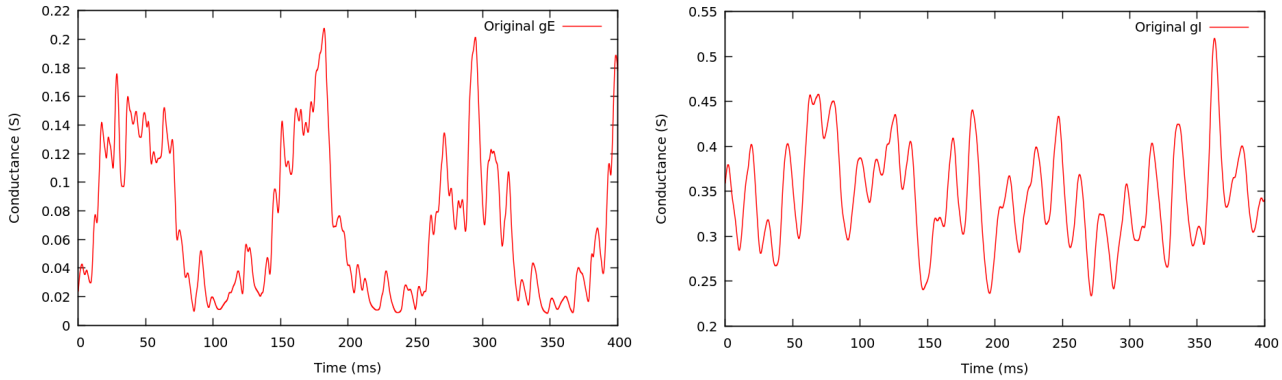

Figure 13: Trajectory of the synaptic conductances g_E and g_I.

Thanks to this, once we get the estimation of the synaptic parameters, we will be able to compare it with the original ones and see if they are a good approximation or not.

To develop this method we have to deal with some differential equations so, we have to use a numerical integrator to integrate the systems 1 and 2. Since we have values of g_E and g_I every 0.01 millisecond (a typical sample step in electrophysiology), we will use a numerical integrator with a constant step. In this case, to simplify the complexity of the algorithm, we have used the simplest one: The forward Euler method.

Using the known data of the synaptic conductances, taking initial conditions for V and the gating variables, and the forward Euler method as the integration method, we can compute the numerical solutions of the membrane potential V and the gating variables. Also, we can compute the original time course trajectory of I_{syn}. It is important to have a basic knowledge of the different behaviour of the membrane potential of a neuron that we could have depending on the different values of I_{app}. Therefore, we integrate the Morris-Lecar and Hodgkin-Huxley models with a synaptic input I_{syn}.

Using the Morris-Lecar equations we know that for $I_{app} \approx 39.96$ we have a Hopf bifurcation: For smaller values of I_{app} the system has a stable fixed point which, at the bifurcation, loses the stability and a periodic

solution appears. In Figure 14, we plot the trajectory of $V(t)$ considering $I_{app} = 30$ and $I_{app} = 45$. As we

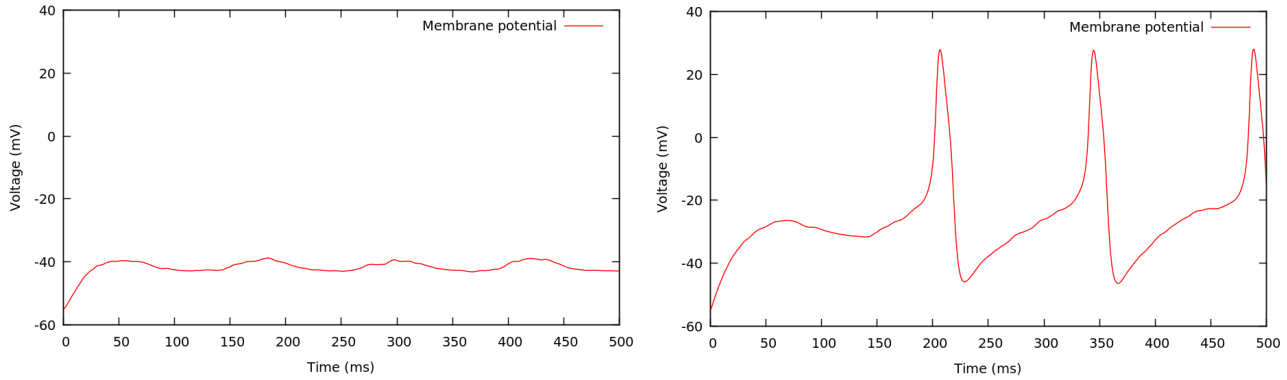

Figure 14: Membrane potential solution of the Morris-Lecar equations with a synaptic input I_{syn} taking $I_{app} = 30$ and $I_{app} = 45$.

can see in the left image of Figure 14, when $I_{app} = 30$, the cell is at rest. There is an stable equilibrium point, $V_{eq} \approx -39mV$, and the voltage will converge at this point. In the right image of Figure 14, when $I_{app} = 45$, we can see the appearance of a stable limit cycle; the membrane potential oscillates and we can identify the action potentials.

The same happens with the reduced Hodgkin-Huxley model. For $I_{app} \approx 6.7$ we have also a Hopf bifurcation. As in Figure 14, in the left image of Figure 15 we can see the subthreshold behaviour of the

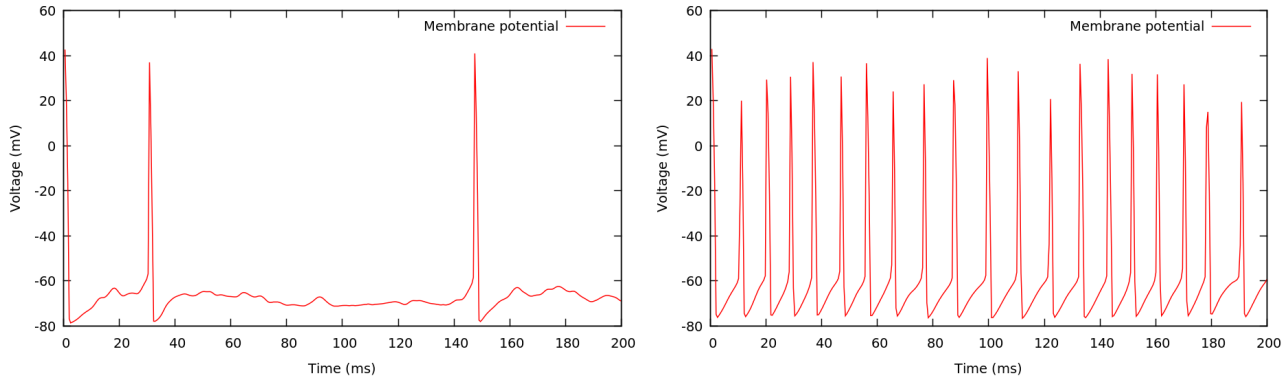

Figure 15: Membrane potential solution of the reduced Hodgkin-Huxley equations with a synaptic input I_{syn} taking $I_{app} = 0$ and $I_{app} = 20$

membrane potential, and at the right image we can see the periodic solutions and the oscillatory behaviour of the voltage.

4.1 Estimation of I_{syn}

In Chapter 3 we have seen that to estimate the synaptic current I_{syn}, we start copying the model and obtaining a new dynamics for $(\hat{V}, \hat{w})$ or $(\hat{V}, \hat{n})$ (depending if we are working with the Morris-Lecar equations or the reduced Hodgkin-Huxley model), replacing the synaptic input I_{syn} by a new variable u (equations 5 and 7). After computing the dynamics of the membrane potential error (e_V) and the gating-variable error $(e_w$ or $e_n)$, we define u so that the errors converge to zero. We have proven that the gating-variable error has a fast convergence to zero, see Figure 16.

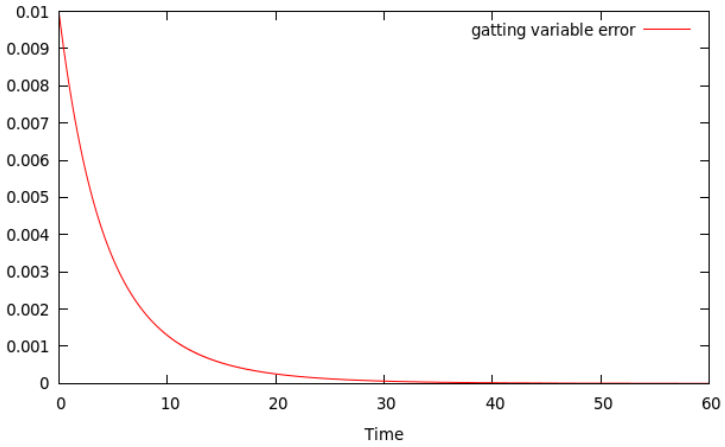

Figure 16: Fast convergence of the gating-variable error (e_w) for the Morris-Lecar model.

In the computational case, to impose that e_V converges to zero let's define the hysteresis $\varepsilon_{hys} = 0.01$ and the open set $\mathcal{H} = (-\varepsilon_{hys}, \varepsilon_{hys})$. Using a control action we will force e_V to converge into it.

Assuming that the integration time set is $\{t_0, t_1, ..., t_N\}$, given $n \in [0, N] \cap \mathbb{N}$ we have that:

- If $e_V(t_n) \in \mathcal{H}$ and $e_V(t_{n+1}) > \varepsilon_{hys}$, using an interpolation we look for $t^* \in (t_n, t_{n+1})$, such that $e_V(t^*) = \varepsilon_{hys}$, we impose that $\frac{de_V(t^*)}{dt} < 0$ and integrate until t_{n+1} again.
- If $e_V(t_n) \in \mathcal{H}$ and $e_V(t_{n+1}) < -\varepsilon_{hys}$, using an interpolation we look for $t^* \in (t_n, t_{n+1})$, such that $e_V(t^*) = -\varepsilon_{hys}$, we impose that $\frac{de_V(t^*)}{dt} > 0$, and integrate until t_{n+1} again.

We repeat these steps until we get that $e_V(t_{n+1}) \in \mathcal{H}$.

In Figure 17 we can see an examples of the plots e_V to understand the control action.

A more general plot of $e_v(t)$, integrating until $T_{max} = 200ms$ and plotting only some of the points of the trajectory, is seen in Figure 18. This shows that $e_v(t) \in \mathcal{H}$ for $t \in [0, T_{max}]$.

In the previous chapter, we have seen that the dynamic of e_V is controlled by the function u. So, as we have seen above, if $e_V(t_n) \in \mathcal{H}$ and $e_V(t_{n+1}) \notin \mathcal{H}$, at instant t^* we have to define $u(t^*)$ in order to have $\frac{de_V(t^*)}{dt} < 0$ or $\frac{de_V(t^*)}{dt} > 0$ depending on the value of $e_V(t_{n+1})$.

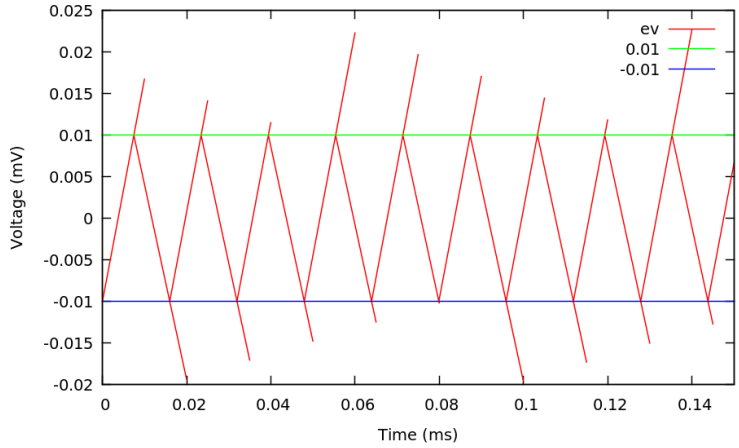

Figure 17: Plot of the membrane potential error when $I_{app} = 45$ and $C = 20$.

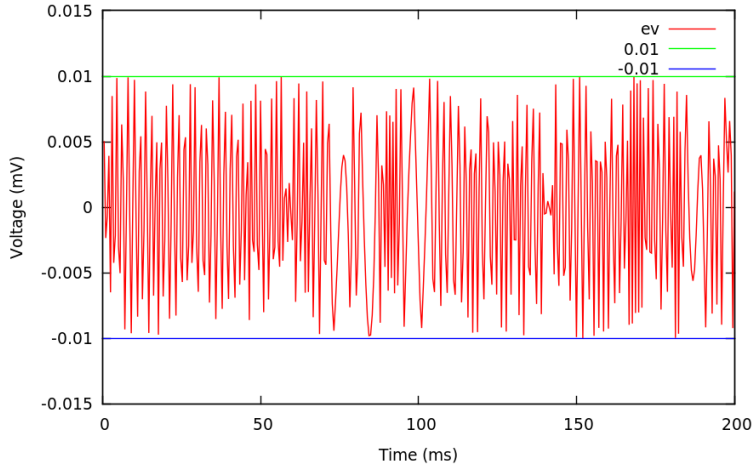

Figure 18: Plot of the membrane potential error when $I_{app} = 45$ and $C = 1$.

The dynamic of e_V using the Morris-Lecar equations, is the following:

$$C\dot{e_v} = -\bar{g_K} e_w (V - V_K) + I_{syn} - u$$

If we have that $e_V(t_{n+1}) > \varepsilon_{hys}$, we want:

$$\frac{-\bar{g_K} e_w(t^*)(V(t^* - V_K) + I_{syn}(t^*) - u(t^*)}{C} < 0$$

or, equivalently,

$$u(t^*) + \bar{g_K} e_w(t^*)(V(t^*) - V_K) > I_{syn}(t^*)$$

Denoting M_{syn} as the maximum value of I_{syn}, and imposing that $u(t^*) = M_{syn} - \bar{g_K} e_w(t^*)(V(t^*) - V_K)$, then the condition is reached and $\frac{de_v(t^*)}{dt} < 0$.

If $e_V(t_{n+1}) < -\varepsilon_{hys}$, we define $u(t^*)$ so that:

$$u(t^*) + \bar{g_K} e_w(t^*)(V(t^*) - V_K) < I_{syn}(t^*)$$

Denoting m_{syn} as the minimum value of I_{syn}, and imposing $u(t^*) = m_{syn} - \bar{g_K} e_w(t^*)(V(t^*) - V_K)$, then the condition is reached and $\frac{de_v(t^*)}{dt} < 0$.

Now, in both cases, we integrate from t^* until t_{n+1}:

$$e_V(t_{n+1}) = e_V(t^*) + (t_{n+1} - t^*)\frac{de_V(t^*)}{dt}$$

- If $e_v(t_{n+1}) \notin \mathcal{H}$, then we have to repeat the process.
- If $e_v(t_{n+1}) \in \mathcal{H}$, then we have that $u(t_{n+1}) = u(t^*)$.

In the case that for some value of n, $e_v(t_n) \in \mathcal{H}$ and $e_v(t_{n+1}) \in \mathcal{H}$, then we have that $u(t_{n+1}) = u(t_n)$.

Let us plot the trajectory of $u(t)$ in order to check the previous assumptions. In the Morris-Lecar model, we choose $M_{syn} = 50$ and $m_{syn} = -50$, see Figure 19.

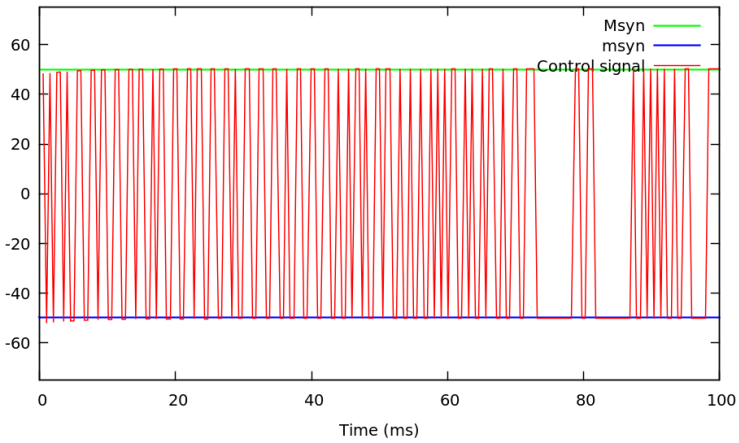

Figure 19: Plot of the trajectory $u(t)$ for the Morris-Lecar model with $I_{appa} = 45$.

An analogous definition for u is done when we use the Hodgkin-Huxley equations instead of the Morris-Lecar model. We are not going to explain it, but notice that using this model we take $M_{syn} = 19$ and $m_{syn} = -59$.

Filtering the input $u(t)$ we expect to obtain an approximation of the original synaptic current I_{syn}. We will denote with $\hat{I}_{syn}$ the trajectory of this estimated function. We have computed this new function using the Morris-Lecar equations and the reduced Hodgkin-Huxley model. In Figures 20 and 21, we compare the trajectory of the original synaptic current with the estimated one.

In Figure 20 we can see the estimation of the function I_{syn} using the Morris-Lecar model. It is clear that $\hat{I}_{syn}$ is a good approximation, and the behaviour of the estimated function is similar to the original one.

The same happens with the estimation of the function I_{syn} using the reduced Hodgkin-Huxley equations, see Figure 21.

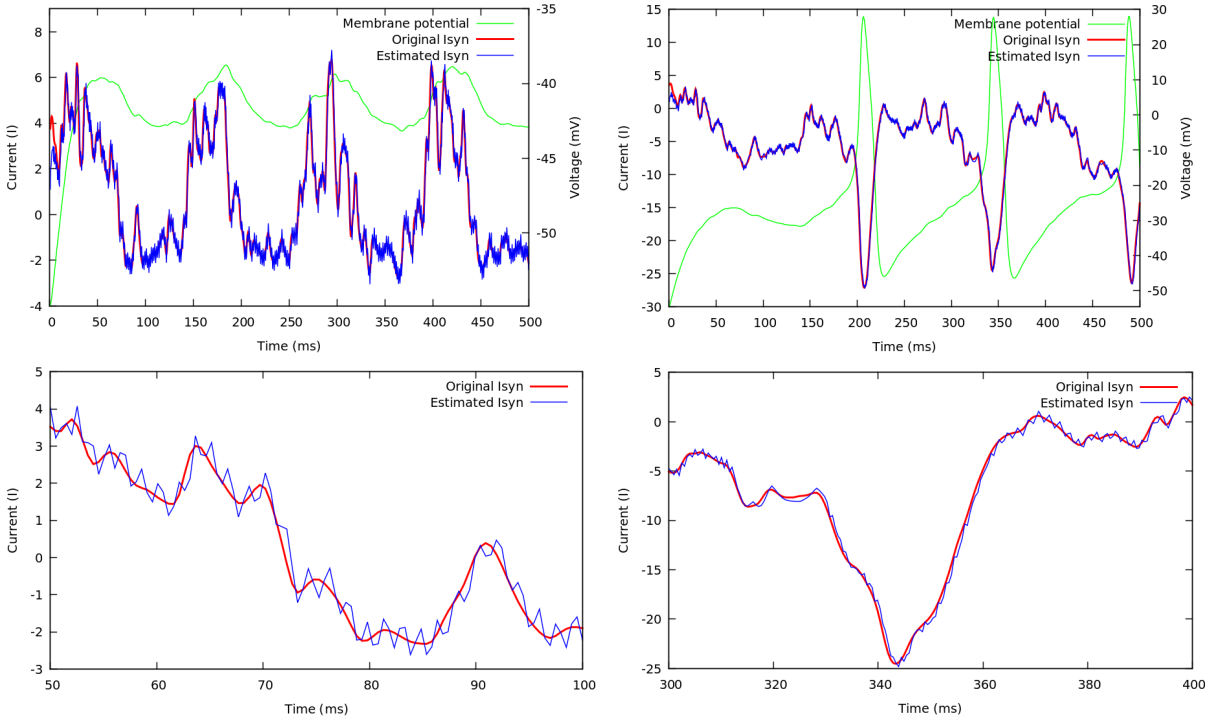

Figure 20: Comparison between $\hat{I}_{syn}$ and I_{syn} from Morris-Lecar equations using $I_{app} = 30$ and $I_{app} = 45$.

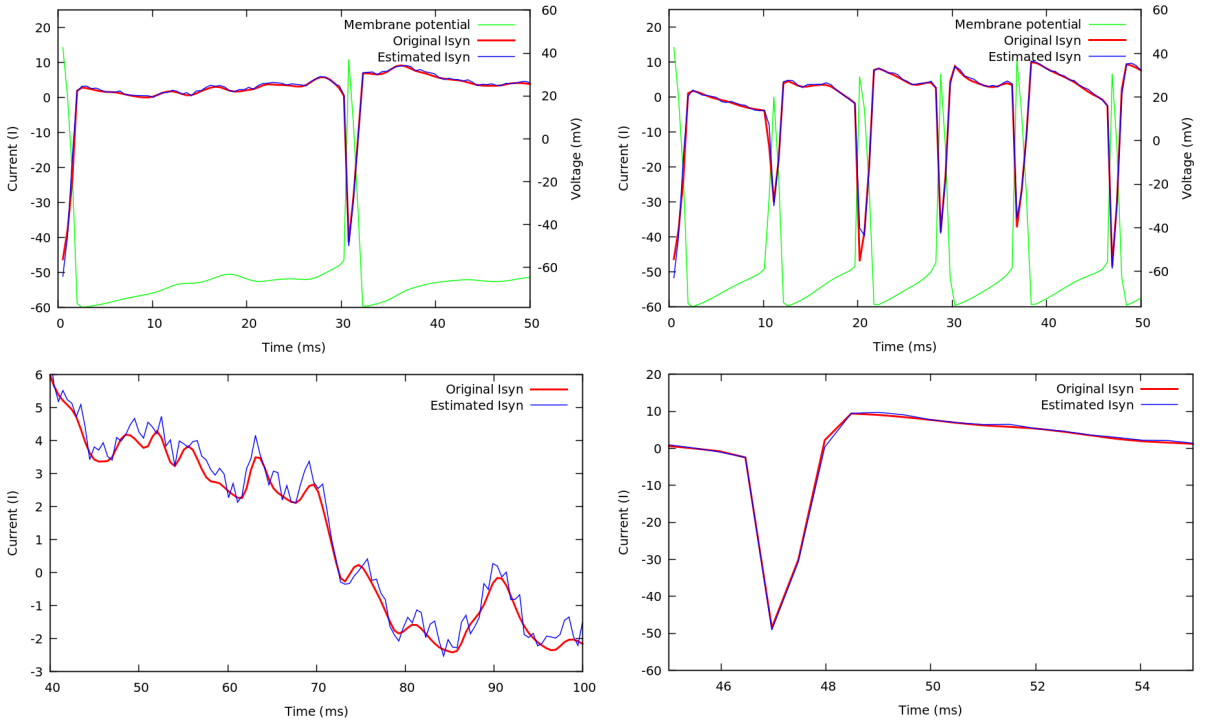

Figure 21: Comparison between $\hat{I}_{syn}$ and I_{syn} from Hodgkin-Huxley equations using $I_{app} = 0$ and $I_{app} = 20$.

To compare numerically the functions $\hat{I}_{syn}$ and I_{syn} we can compute the error between the two trajectories. We will compute the *root mean square error* between them.

Assuming that I_{syn} and $\hat{I}_{syn}$ are evaluated at t_n $\forall n \in [0, N] \cup \mathbb{N}$, and denoting $I_{syn}(t_n) = I_{syn_n}$ and $\hat{I}_{syn}(t_n) = \hat{I}_{syn_n}$, we will be able to compute the square mean square error as:

$$RMSE(\hat{I}_{syn}) = \sqrt{\frac{1}{N}\sum_{n=0}^{N}(I_{syn_n} - \hat{I}_{syn_n})^2}.$$

The relative RSME can be computed in the following way:

$$relRSME(\hat{I}_{syn}) = \frac{RMSE}{M_{syn} - m_{syn}}$$

Let us compute this error for the previous trajectories. Using the Morris-Lecar model we obtain that:

- With $I_{app} = 30$ we have that $RMSE(\hat{I}_{syn}) = 0.341$ and $relRMSE(\hat{I}_{syn}) = 3.73 \cdot 10^{-2}$.
- With $I_{app} = 45$ we have that $RMSE(\hat{I}_{syn}) = 0.425$ and $relRMSE(\hat{I}_{syn}) = 1.38 \cdot 10^{-2}$.

Using the Hodgkin-Huxley equations we obtain that:

- With $I_{app} = 0$ we have that $RMSE(\hat{I}_{syn}) = 0.493$ and $relRMSE(\hat{I}_{syn}) = 8.79 \cdot 10^{-3}$.
- With $I_{app} = 20$ we have that $RMSE(\hat{I}_{syn}) = 1.009$ and $relRMSE(\hat{I}_{syn}) = 1.48 \cdot 10^{-2}$.

We can see that the used method gives a good approximation of the synaptic current I_{syn}, but there is a small error that has to be studied in order to improve our method. In the following chapter we will try to understand this error and reduce it.

We have to notice that, in the experimental case, it is not possible to compare the estimated function $\hat{I}_{syn}$ with the original (because we do not know it). This means that we will not be able to analyze this error in the estimated function $\hat{I}_{syn}$ comparing it with the original synaptic current, and as consequence, we can not reduce it. Hence, this computation has to be interpreted as a prospective computational experiment to assess how much the estimation is wrong because of this lag.

However, knowing that, in the experimental case we have as input the membrane potential trajectory V, we can get the original trajectory of w and we will be able to compute $\hat{I}_{syn}$ with the explained method.

Knowing this obtained function $\hat{I}_{syn}$, we can integrate the following system:

$$\begin{cases} C\dot{\hat{V}} = I_{app} - \bar{g}_{\mathrm{K}}\hat{w}(\hat{V} - V_{\mathrm{K}}) - \bar{g}_{Ca}m_{\infty}(V)(\hat{V} - V_{\mathrm{Ca}}) - g_L(\hat{V} - V_L) - \hat{I}_{syn} \\ \dot{\hat{w}} = \phi(\frac{w_{\infty}(\hat{V}) - \hat{w}}{\tau_w(\hat{V})}) \end{cases}$$

and compute the trajectory of $\hat{V}$ using as initial conditions $\hat{V}_0 = V_0$ and $\hat{w}_0 = w_0$ where (V_0, w_0) are points of the original trajectory of V and w.

So, comparing the trajectories of V and $\hat{V}$ we will be able to see if $\hat{I}_{syn}$ is a good approximation of the original synaptic current. Let's analyze the error.

4.2 Correction of Isyn

Looking at Figures 20 and 21, we can see that there is a lag in the estimated function with respect to the original I_{syn}, see Figure 22.

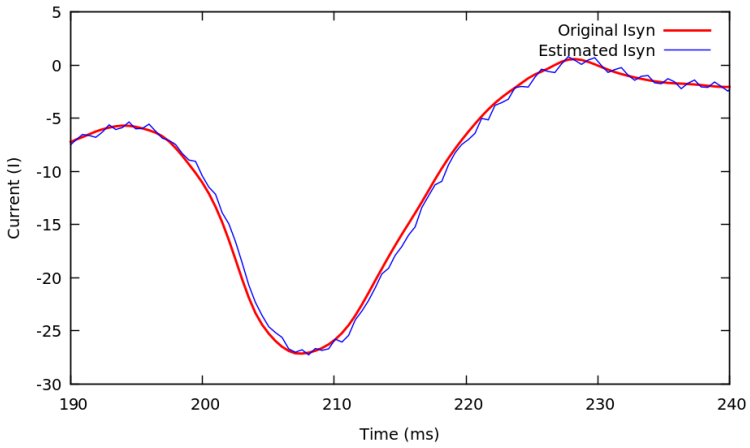

Figure 22: Spike region of the estimation of I_{syn} using the Morris-Lecar equations respect to the original function. We can see that the estimated function is a little behind of time compared to the original.

In order to go in depth in the causes of this lag, let us consider an idealized sinusoidal signal. If we solve a linear system of ODEs with a sinusoidal excitation ($a\sin(\omega t)$), we will obtain as a solution a sinus signal with the same frequency as the input, different amplitude, and with a small lag. This solution is a linear combination of trigonometric functions with the same frequency and the solution can be written as:

$$x(t) = b\sin(\omega t + \varphi)$$

We can see an example of this solution in Figure 23.

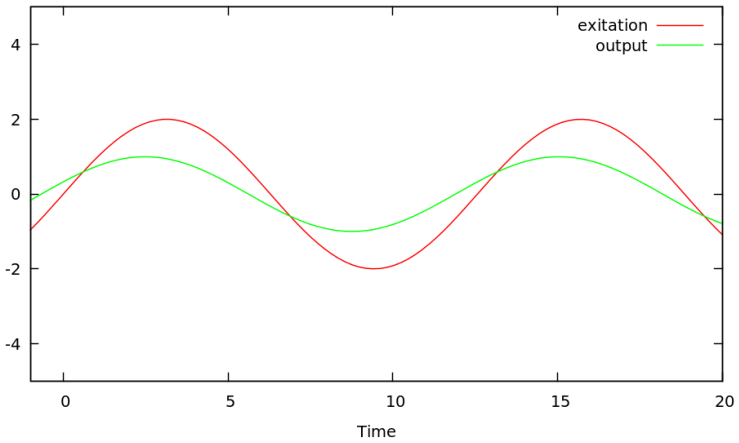

Figure 23: Comparison between the excitation and the solution of the linear system. We have taken $\omega = \frac{1}{2}$, $a = 2$, $b = 1$ and $\varphi = \frac{1}{3}$.

In our algorithm, we have, as input, the excitatory and inhibitory synaptic parameters, and with them, we can recreate the synaptic term I_{syn}. If we decompose this signal in a Fourier series, we have some frequencies that will define our original input.

We know that to obtain an estimation of this signal, $\hat{I}_{syn}$ we define the variable u and we apply a linear filter:

$$\frac{d}{dt}\hat{I}_{syn} = -\frac{\hat{I}_{syn} - u}{\tau_y}$$

If we consider the function I_{syn} as a Fourier series, we have a set of frequencies and, in fact, we are applying this filter at each one. Therefore, as output we will have a lag for each frequency. This induces a small lag of the estimated I_{syn} compared with the original signal. However, the differential equation itself, generates the general lag on the responses for the same reason explained above. The lag induced by the filter is secondary.

To have a better estimation of the synaptic term I_{syn}, we will try to correct this small lag. We will construct this correction method for the Morris-Lecar model, but as above, the argument for the reduced Hodgkin-Huxley equations is analogous and we are not going to focus on it. In this chapter we want to explorer if this observable lags are the main responsible for the error between I_{syn} and $\hat{I}_{syn}$. As we have said above we will try to correct this lag working with V and $\hat{V}$.

In our algorithm, we have as input the synaptic conductances and we can use them to compute the trajectory of V using the forward Euler method as integration method. With the same integration method we compute the trajectory of $\hat{V}$ in order to have the functions V and $\hat{V}$ evaluated at the same time values. Comparing the trajectories of V and $\hat{V}$ we will be able to see if we have a lag between these two functions. In Figure 24 we can see the plot of the comparison between the two trajectories. In this case, we have integrated until $T_{Max} = 400ms$ and the root mean square error of two functions is $RMSE(\hat{V}) = 0.9334$.

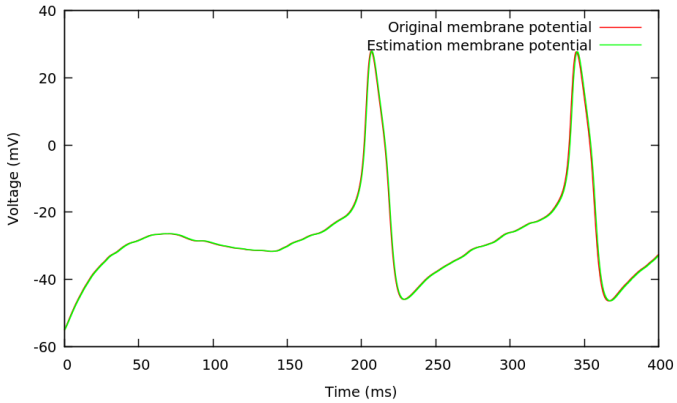

Figure 24: Comparison between V and $\hat{V}$.

In Figure 25 we can see the trajectories of the two functions at the first spike. It is clear that the lag between the two functions is similar to the lag between I_{syn} and $\hat{I}_{syn}$. We will try to correct the estimated synaptic trajectory correcting the lag between the trajectories of the voltage.

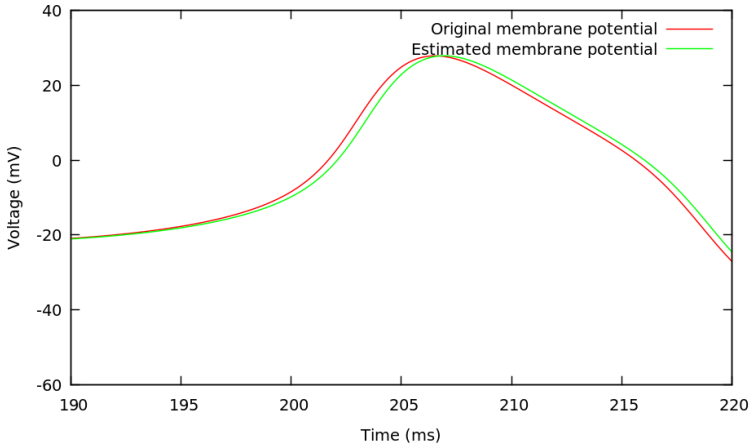

Figure 25: Comparison between V and $\hat{V}$, first spike.

Having a lag between two trajectories means that, $\forall t$, $\exists \Delta_t$ such that $\hat{V}(t - \Delta_t) = V(t)$. It can be seen that the lag in Figure 25 is similar to the lag in Figure 26 so we will assume that $\Delta_t = \Delta \ \forall t$.

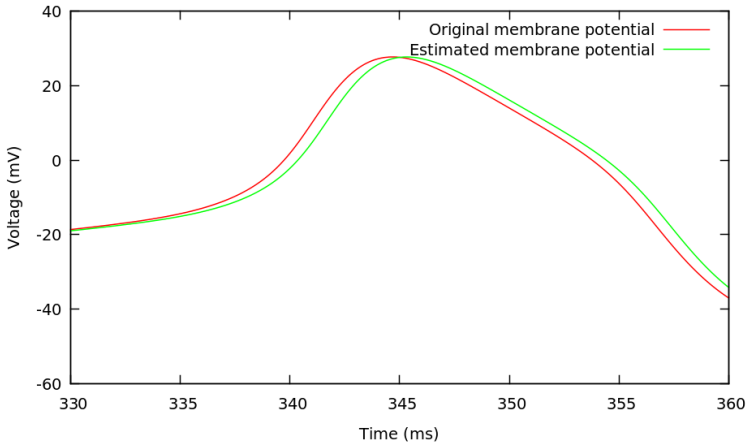

Figure 26: Comparison between V and $\hat{V}$, second spike.

With that, we conclude that given the trajectories of V and $\hat{V}$, exists a parameter $\Delta \geq 0$ that for every value of t, $\hat{V}(t) = V(t - \Delta)$.

To correct the trajectory of $\hat{V}$ we will give different values to this new parameter $\Delta \geq 0$, and for each Δ we define a new function $\hat{V}_\Delta$.

Given a value for Δ, we will define $\hat{V}_\Delta$ in the following way:

$$\hat{V}_\Delta(t) = \hat{V}(t + \Delta) \ , \forall t \geq 0.$$

After finding this new trajectory we can compute, again, the root square mean error between $\hat{V}_\Delta(t)$ and the original trajectory V. The main goal of this part is to find the optimum value for Δ for which the error

between the voltages is minimal.

Some computations shows us that for $\Delta = 0.52$ ms, we have the minimal error with value $RMSE(\hat{V}_\Delta) = 0.211$. In Figure 27 we compare the original and the corrected trajectories. As we can see, we have reduced the original root square mean error from $RMSE(\hat{V}_0) = 0.9334$ to $RMSE(\hat{V}_{0.52}) = 0.211$.

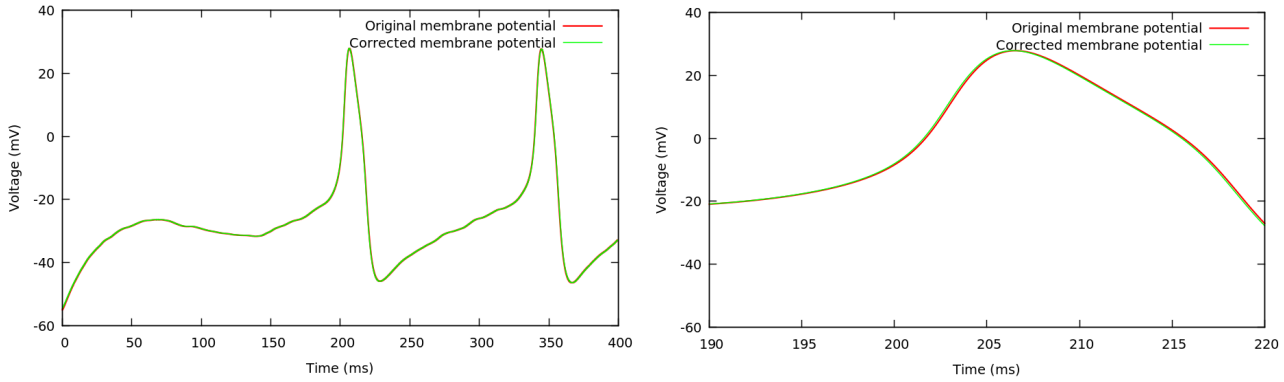

Figure 27: Comparison between the original voltage V and the corrected estimated voltage $\hat{V}_\Delta$.

Using the same argument as above, we can compute the corrected function $\hat{I}^\Delta_{syn}$ using the previous assumption:

$$\hat{I}^\Delta_{syn}(t) = \hat{I}_{syn}(t + \Delta)$$

We will compute this new function using that $\Delta = 0.52ms$ because is the optimal Δ that reduce the error.

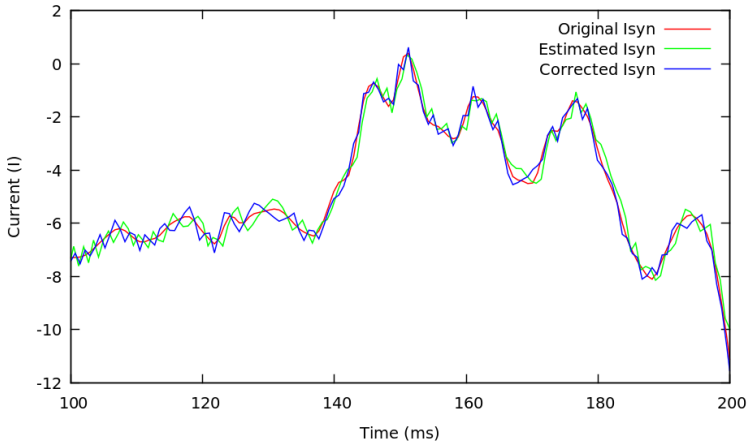

Figure 28: Comparison between I_{syn}, $\hat{I}_{syn}$, and the corrected function $\hat{I}^\Delta_{syn}$.

Figure 28 shows the comparison between the three trajectories of the synaptic current: the original, the estimated and the corrected one. It can be seen that the lag that we had before is reduced and we have a better approximation of the synaptic term I_{syn}.

Even if we have improved the estimation of I_{syn} we can deduce that the root square mean error between the two trajectories will not be close enough to zero. Notice that minimal error between the voltages is $RMSD(\hat{V}_\Delta) = 0.211$, so we only have divided the original error by 4, so, it means that aldought we have corrected the lag between I_{syn} and $\hat{I}_{syn}$, there exists an important error between these two functions.

We have commented that the observable lag from above is generated principally for the action of the differential equation (as a filter) from the model and secondary for the use of the linear filter for the estimation of $\hat{I}_{syn}$. Therefore if we would like to minimize the actual error we could change the actual linear filter for a more complex one. We should use a superior order filter. However the main goal of this project is not the design of superior order filters and the use of it so, we are going to try to distinguish the synaptic conductances from the actual estimation of I_{syn}.

Now we check if this approximation of I_{syn} is closer enough to the original one to find a good estimation of the synaptic conductances $g_E(t)$ and $g_I(t)$.

4.3 Estimation of the synaptic conductances.

Our goal is to deduce the expression of $\hat{g}_E$ and $\hat{g}_I$ from the equation of the synaptic current:

$$\hat{I}_{syn}(t) = -\hat{g}_E(t)(V(t) - V_E) - \hat{g}_I(t)(V(t) - V_I)$$

where $\hat{I}_{syn}$ is the trajectory of the synaptic term estimated before. As we have two unknowns and only one equation, we need to construct another equation to solve a linear system. While we are integrating the system, we will consider that these two conductances are constant during two integration steps. With this assumption, and using that the integration times are $t_0, t_1, ..., t_N$, we can construct the following system of equations and solve it to get $\hat{g}_E$ $\hat{g}_I$:

$$\begin{cases} I_{syn_{2n}} = g_{E_{2n}}(V_{2n} - V_E) + g_{I_{2n}}(V_{2n} - V_I) \\ I_{syn_{2n+1}} = g_{E_{2n}}(V_{2n+1} - V_E) + g_{I_{2n}}(V_{2n+1} - V_I) \end{cases} \quad \forall n \in [0, \frac{N-1}{2}] \cap \mathbb{N}.$$

Our algorithm uses as input a known data of the original $g_E(t)$ and $g_I(t)$ trajectories, specifically a file with values of $g_E(t)$ and $g_I(t)$ for every 0.01 milliseconds. In Figure 29 we can see the trajectory of the synaptic conductances g_E and g_I.

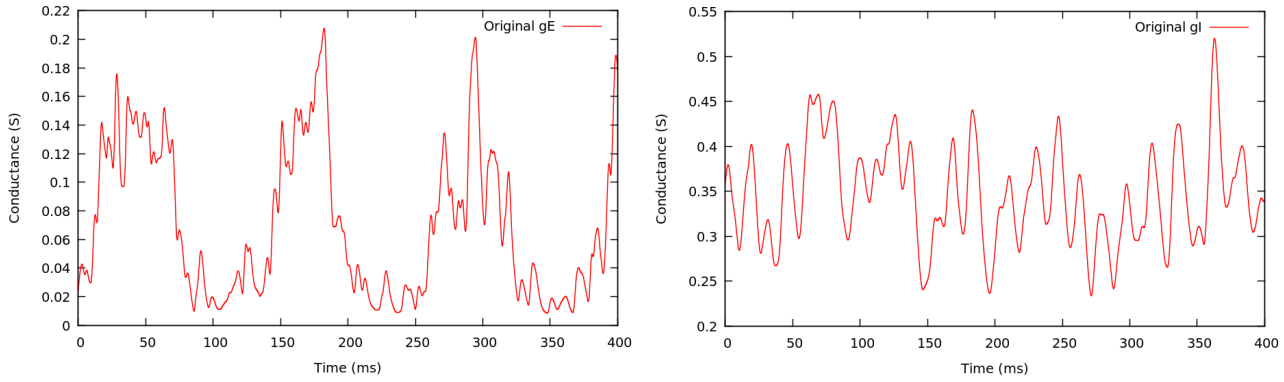

Figure 29: Trajectory of the original synaptic conductances g_E and g_I.

We will integrate our system to compute V and $\hat{I}_{syn}$ with an integration step equal to $\delta = 0.005$ in order to read a value of the original trajectories g_E and g_I every two integration steps.

This means that, considering that the input file we have values of the trajectory of g_E and g_I for this set of times $\{t_0, t_1, ..., t_N\}$, in our integration method we consider that the integration times are $\{t_0, t_\delta, t_1, t_{1+\delta}, ..., t_N, t_{N+\delta}\}$, where $t_{n+\delta} = t_n + \delta$. We will impose that:

$$\begin{cases} g_{E_n} = g_{E_{n+\delta}} \\ g_{I_n} = g_{I_{n+\delta}} \end{cases}, \forall n \in [0, N] \cap \mathbb{N}$$

After computing the trajectory of V and $\hat{I}_{syn}$ we try to estimate the synaptic conductances g_E, g_I solving the previous system:

$$\begin{cases} \hat{I}_{syn_n} = \hat{g}_{E_n}(V_n - V_E) + \hat{g}_{I_n}(V_n - V_I) \\ \hat{I}_{syn_{n+\delta}} = \hat{g}_{E_n}(V_{n+\delta} - V_E) + \hat{g}_{I_n}(V_{n+\delta} - V_I) \end{cases} \quad \forall n \in [0, N] \cap \mathbb{N}$$

In Figure 30 and 31 we can see the comparison between the original and estimated trajectories. It is clear that there is a large difference between the two trajectories, and the amplitude of the estimated synaptic conductances is so much bigger than the original one. Let us see what is happening and also try to explain the oscillatory behavior of the two estimated functions.

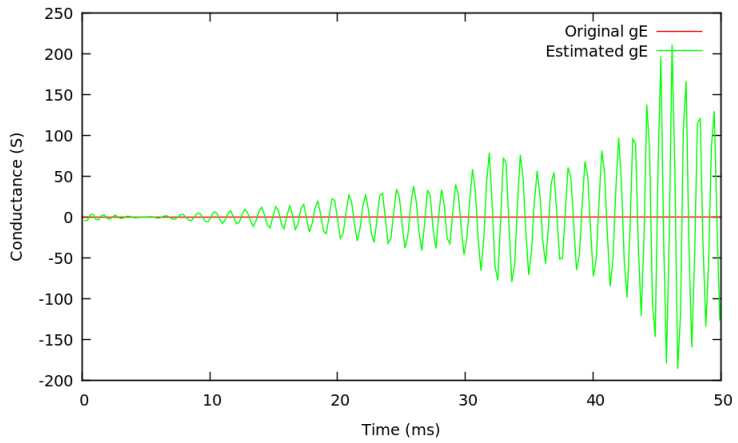

Figure 30: Comparison between the original g_E, and the estimated synaptic conductance $\hat{g}_E$.

It is clear that if we solve the same system of equations but instead of using $\hat{I}_{syn}$ we use the original trajectory of I_{syn}, the solutions that we will obtain will be exactly the trajectory of g_E and g_I because, for every two integration steps, we recuperate the parameters that we have used to construct I_{syn}.

Let us introduce the notation $A_n = -(V_n - V_E)$ and $B_n = -(V_n - V_I)$ that we will use from now on.

As the integration step is so small ($\delta = 0.005$), it is clear that during two integration steps, the trajectory of V will change smoothly, so, $\exists \varepsilon << 1$ such that $\forall n \in [0, N] \cap \mathbb{N}$, $|V_n - V_{n+\delta}| < \varepsilon$, so consecutively $|A_n - A_{n+\delta}| < \varepsilon$ and $|B_n - B_{n+\delta}| < \varepsilon$.

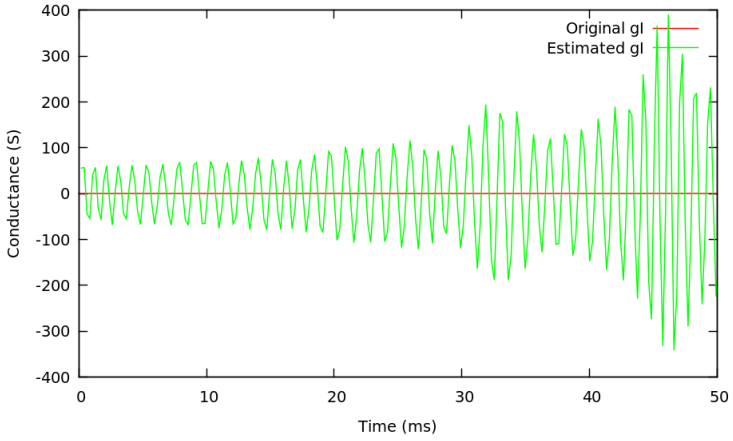

Figure 31: Comparison between the original g_I, and the estimated synaptic conductance $\hat{g}_I$.

The same happens with the original trajectory of I_{syn}; $|I_{syn_n} - I_{syn_{n+\delta}}| < \varepsilon$ for a small value of ε.

On the other hand, because of the control action that we are applying and the simplicity of the filter, we have that the trajectory of $\hat{I}_{syn}$ oscillates around the trajectory of the original trajectory I_{syn}. See it in Figure 32.

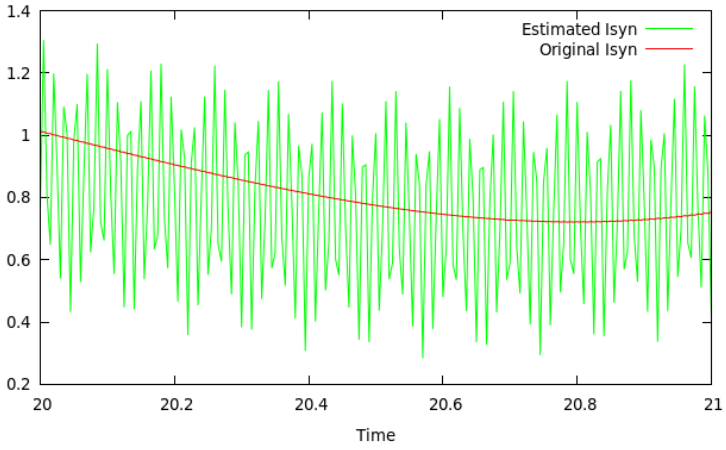

Figure 32: Oscillations of $\hat{I}_{syn}$ around the original trajectory I_{syn}

So, we can see that given $n \in [0, N] \cap \mathbb{N}$, $\exists \varepsilon << 1$ such that $|I_{syn_n} - I_{syn_{n+\delta}}| < \varepsilon$, and $|\hat{I}_{syn_n} - \hat{I}_{syn_{n+\delta}}| >> \varepsilon$.

Let us try to solve the system presented before:

$$\begin{cases} \hat{I}_{syn_n} = A_n \hat{g}_{E_n} + B_n \hat{g}_{I_n} \\ \hat{I}_{syn_{n+\delta}} = A_{n+\delta} \hat{g}_{E_n} + B_{n+\delta} \hat{g}_{I_n} \end{cases}, \forall n \in [0, N]$$

so,

$$\hat{g}_{I_n} = \frac{\hat{I}_{syn_n} - A_n \hat{g}_{E_n}}{B_n}$$

$$\hat{g}_{I_n} = \frac{\hat{I}_{syn_{n+\delta}} - A_{n+\delta} \hat{g}_{E_n}}{B_{n+\delta}}$$

We can equalize the two equations:

$$\frac{\hat{I}_{syn_n} - A_n \hat{g}_{E_n}}{B_n} = \frac{\hat{I}_{syn_{n+\delta}} - A_{n+\delta} \hat{g}_{E_n}}{B_{n+\delta}}$$

$$B_{n+\delta} \left(\hat{I}_{syn_n} - A_n \hat{g}_{E_n} \right) = B_n \left(\hat{I}_{syn_{n+\delta}} - A_{n+\delta} \hat{g}_{E_n} \right)$$

and finally we get:

$$\hat{g}_{E_n} = \frac{B_{n+\delta} \hat{I}_{syn_n} - B_n \hat{I}_{syn_{n+\delta}}}{B_{n+\delta} A_n - B_n A_{n+\delta}}$$

We can do the same using now the original values of I_{syn} we have that:

$$g_{E_n} = \frac{B_{n+\delta} I_{syn_n} - B_n I_{syn_{n+\delta}}}{B_{n+\delta} A_n - B_n A_{n+\delta}}$$

Now let us compute the difference between g_{E_n} and $\hat{g}_{E_n}$.

$$g_{E_n} - \hat{g}_{E_n} = \frac{B_{n+\delta}(I_{syn_n} - \hat{I}_{syn_n}) - B_n(I_{syn_{n+\delta}} - \hat{I}_{syn_{n+\delta}})}{B_{n+\delta} A_n - B_n A_{n+\delta}}$$

Using that $|B_n - B_{n+\delta}| < \varepsilon$, we will assume that $B_n \approx B_{n+\delta}$, and with that:

$$g_{E_n} - \hat{g}_{E_n} = \frac{B_n(I_{syn_n} - I_{syn_{n+\delta}} - \hat{I}_{syn_n} + \hat{I}_{syn_{n+\delta}})}{B_n(A_n - A_{n+\delta})} = \frac{I_{syn_n} - I_{syn_{n+\delta}} - \hat{I}_{syn_n} + \hat{I}_{syn_{n+\delta}}}{A_n - A_{n+\delta}}$$

Since $|A_n - A_{n+\delta}| < \varepsilon$, $|I_{syn_n} - I_{syn_{n+\delta}}| < \varepsilon$ and $|\hat{I}_{syn_n} - \hat{I}_{syn_{n+\delta}}| >> \varepsilon$, we will have that $|g_{E_n} - \hat{g}_{E_n}|$ will be very large for every value of n. Something similar happens for g_I, and this explains the large amplitude of the trajectories of g_E and g_I.

Also, it is clear that the oscillatory behaviour of the two trajectories comes from the oscillatory behaviour of the estimated function $\hat{I}_{syn}$. In Figure 33 we can see the comparison between $\hat{I}_{syn}$ and the synaptic conductances to compare the oscillatory behaviour of both.

It can be seen that the trajectories of g_E and g_I will be oscillating around zero. This happens because during these two integration steps the trajectory of $\hat{I}_{syn}$ can be growing or decreasing, therefore:

- If the trajectory of $\hat{I}_{syn}$ is growing: $\hat{I}_{syn_n} < \hat{I}_{syn_{n+\delta}}$
- If the trajectory of $\hat{I}_{syn}$ is decreasing: $\hat{I}_{syn_n} > \hat{I}_{syn_{n+\delta}}$

These two options will give us the oscillatory behavior around zero of the synaptic conductances.

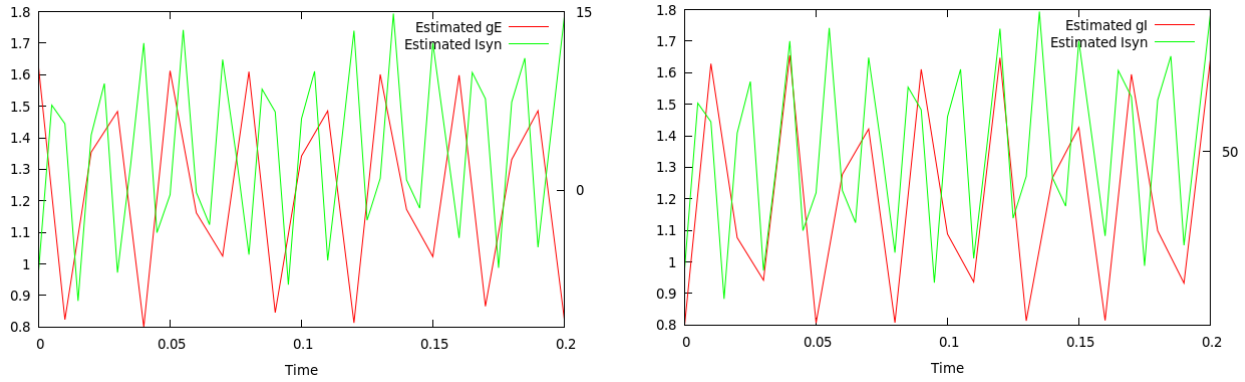

Figure 33: Comparison between the oscillatory behaviour of $\hat{I}_{syn}$ with the oscillatory behaviour of $\hat{g}_E$ and $\hat{g}_I$.

4.3.1 Least square method

After doing these computations we can conclude that the method to differentiate the synaptic conductances explained previously is not efficient enough and we do not reach satisfactory solutions. Observe that the problem appears when we try to use the estimated function $\hat{I}_{syn}$ as input to solve the linear system with the small step $\delta = 0.005$.

To reduce the error, we can try to assume that the synaptic conductances are constant in a larger number of integration steps. Looking at the original trajectories of g_E and g_I we can see that using $\delta = 1$ as period, the trajectories do not change abruptly, so, in our algorithm we will consider that g_E and g_I are constant during every 1 ms period.

Considering that the original file has as time step 0.01, we will integrate the system of equations using this same integration step, and, using the previous assumptions, we construct a overdetermined system with $1/0.01 = 100$ equations:

$$\begin{cases} \hat{I}_{syn_n} = A_n \hat{g}_{E_n} + B_n \hat{g}_{I_n} \\ \hat{I}_{syn_{n+1}} = A_{n+1} \hat{g}_{E_n} + B_{n+1} \hat{g}_{I_n} \\ \hat{I}_{syn_{n+2}} = A_{n+2} \hat{g}_{E_n} + B_{n+2} \hat{g}_{I_n} \qquad , \forall n \in \{0, 100, 200, 300, ...\} \\ ... \\ \hat{I}_{syn_{n+19}} = A_{n+19} \hat{g}_{E_n} + B_{n+99} \hat{g}_{I_n} \end{cases}$$

To solve the overdetermined system we will use the least-squares method. Solving this system we will have a value of $\hat{g}_E$ and $\hat{g}_I$ for $t \in \{0, 1, 2, 3, ...\}$. In Figure 34 we can see the comparison between the original and estimated synaptic conductances. It is clear that the results have not improved substantially, but the amplitude of the functions is smaller.

On the other hand, it can be seen in Figure 35 that if we reduce the amplitude of the two estimated functions, we have a similarity between the shape of the original and estimated functions. Even if we can see a similarity between the behaviours of the synaptic conductances, it is clear that the solutions are not optimal. It is clear that the error between the functions is so large and we have to assume that the method is no functional.

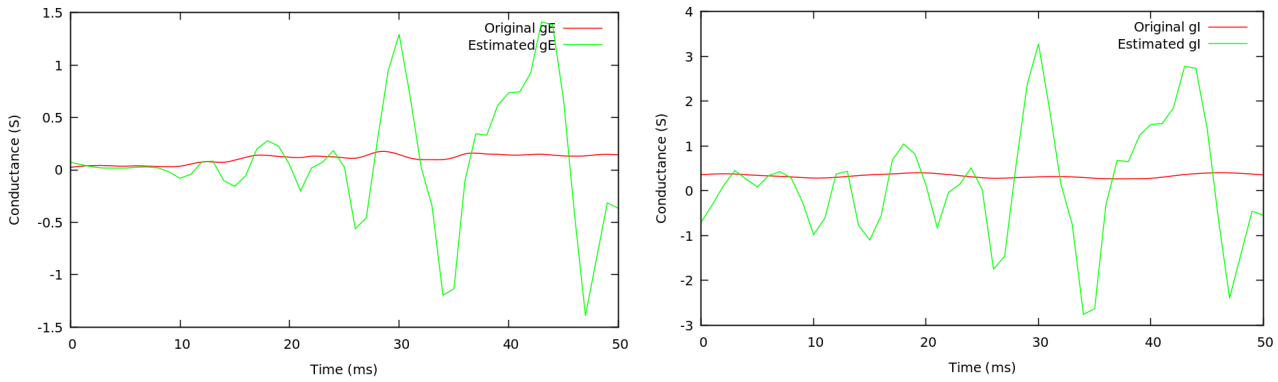

Figure 34: Comparison between the original synaptic conductances and the estimated ones.

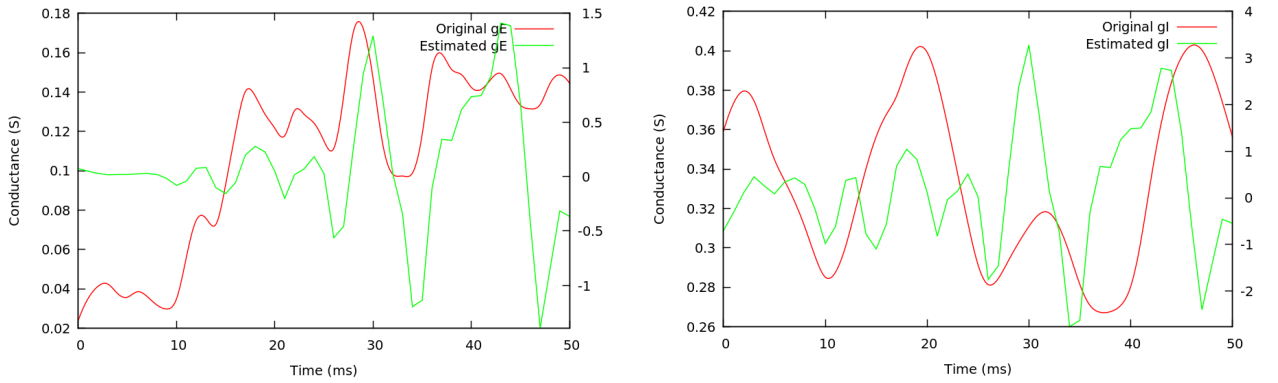

Figure 35: Comparison between the shape of the original synaptic conductances and the estimated ones.

We can conclude that the method explained in this project is useful to estimate the synaptic term I_{syn}. We have seen that the trajectories V and the corrected estimated function $\hat{V}_{\Delta}$ are closer enough to ensure that we have obtained a good copy of the synaptic current I_{syn}. We have to notice that this method is also efficient in the spiking regimes.

The estimated function $\hat{I}_{syn}$ oscillates around the original trajectory of the synaptic term because of the control action applied in the method, and even if we have obtained a good approximation of the synaptic term I_{syn}, the simplicity of the linear filter provokes that the estimation of the synaptic conductances g_E and g_I are very far to the original ones.

The method could be further improved by applying a higher order filter to reduce the small fluctuations of the I_{syn} estimation, which propagate dramatically in the estimation of the conductances.

4.4 Alternative synaptic parameter estimation method

In the previous chapters, we have concluded that using the control method presented in this project, even if the main idea of the method and the theoretical background are consistent, we have not obtained the expected results. The failure with the results of the method presented above force us to search for an

alternative method to estimate the synaptic conductances from experimental data.

In this chapter, we will present a new method assuming that, as above, we have an observable data of the membrane potential of a neuron.

Before presenting the method, we have to notice that the idea of this algorithm for the estimation of the synaptic conductances is similar to the idea of the method explained above of solving a linear system assuming the invariance of the synaptic conductances along a small period of time. But, even if they are similar in this aspect, this new method is not based on control theory as the previous one.

Also like the first method, the new algorithm is also extremely dependent on the model. We will explain the algorithm using the Morris-Lecar equations. As always, we will have an analogous algorithm for the reduced Hodgkin-Huxley model.

This method is inspired in the oversampling method to extract excitatory and inhibitory conductances from single-trial membrane potential recordings presented by Claude Bédard, Alain Destexhe. For more details, see [1].

We have as input an observable data of the membrane potential of a neuron. Assuming that the time set where V is evaluated is $\{t_0, t_1, t_2, ..., t_N\}$, with a constant time step, we have as input a set of values of the trajectory of the voltage V, $\{V_0, V_1, V_2, ..., V_N\}$, where $V_n = V(t_n)$, $\forall n \in [0, N] \cap \mathbb{N}$.

Knowing the trajectory of the voltage, using the Morris-Lecar equations we are able to compute the trajectory of the gating variable w, integrating the following differential equation:

$$\begin{cases} \dot{w} = \phi(\frac{w_\infty(V)-w}{\tau_w(V)}) \\ w(t_0) = w_0 \end{cases}$$

Integrating with a constant step method as the Euler method, the output of this integration will be the following set $\{w_0, w_1, w_2, ..., w_N\}$.

Using the knowing trajectory $\{(V_n, w_n)\}_{n\in[0,N]\cap\mathbb{N}}$ we compute the synaptic conductances. As the control method that we have presented, we will assume that the synaptic conductances are constant along two time steps. This means that for $n = 2i$, $\forall i \in [0, \frac{N-1}{2}] \cap \mathbb{N}$:

$$g_{E\,n} = g_{E\,n+1}$$

$$g_{I\,n} = g_{I\,n+1}$$

So, as output, we expect to obtain the set $\{g_{E0}, g_{E2}, g_{E4}, ..., g_{E\,N-1}\}$, and the set $\{g_{I0}, g_{I2}, g_{I4}, ..., g_{I\,N-1}\}$. Let's explain how to obtain this results.

First of all we have to assume that the trajectory of the voltage can be integrated using the Morris-Lecar equations. This means that the input voltage is the solution of the following differential equation:

$$\begin{cases} C\dot{V} = I_{app} - \bar{g_{\mathrm{K}}} w(V - V_{\mathrm{K}}) - \bar{g_{Ca}} m_\infty(V)(V - V_{\mathrm{Ca}}) - g_L(V - V_L) - I_{syn} \\ \dot{w} = \phi(\frac{w_\infty(V)-w}{\tau_w(V)}) \end{cases}$$

This means that, if we integrate the previous differential equation with a constant step integration method, using as initial conditions $V(t_0) = V_0$ and $w(t_0) = w_0$ and the constant time step $\delta = t_{i+1} - t_i$,

$\forall i \in [0, N-1]$, we have to obtain a trajectory similar to the original input. So, using the Euler discretization, we have that:

$$V_n = V_{n-1} + \delta f(V_{n-1}, w_{n-1})$$

where V_n and V_{n-1} are input values of the voltage, and δ is the constant time step, and f is the Morris-Lecar differential equation.

Using that, we can define this system of equations:

$$\begin{cases} V_{n+1} = V_n + \delta f(V_n, w_n) \\ V_{n+2} = V_{n+1} + \delta f(V_{n+1}, w_{n+1}) \end{cases}$$

where we known the values of V_n, V_{n+1} and V_{n+2}, and w_n, w_{n+1} and w_{n+2}.

Assuming that the voltage follows the Morris-Lecar equations, we have that:

$$f(V_n, w_n) = \frac{1}{C}\left[f_1(V_n, w_n) - I_{syn_n}\right]$$

where:

$$f_1(V_n, w_n) = I_{app} - \bar{g_{\mathrm{K}}} w_n (V_n - V_{\mathrm{K}}) - \bar{g_{Ca}} m_\infty(V)(V_n - V_{\mathrm{Ca}}) - g_L(V_n - V_L)$$

So, we have that:

$$\begin{cases} V_{n+1} = V_n + \frac{\delta}{C}\left[f_1(V_n, w_n) - I_{syn_n}\right] \\ V_{n+2} = V_{n+1} + \frac{\delta}{C}\left[f_1(V_{n+1}, w_{n+1}) - I_{syn_{n+1}}\right] \end{cases}$$

Now, using the synaptic current equation:

$$I_{syn_n} = -g_{E\,n}(V_n - VE) - g_{I\,n}(V_n - VI)$$

and assuming that the synaptic conductances are constant along two time steps, we will have finally the following system of equations:

$$\begin{cases} V_{n+1} = V_n + \frac{\delta}{C}\left[f_1(V_n, w_n) + g_{E\,n}(V_n - VE) + g_{I\,n}(V_n - VI)\right] \\ V_{n+2} = V_{n+1} + \frac{\delta}{C}\left[f_1(V_{n+1}, w_{n+1}) + g_{E\,n}(V_{n+1} - VE) + g_{I\,n}(V_{n+1} - VI)\right] \end{cases}$$

with $g_{E\,n}$, $g_{I\,n}$ as unknowns.

If we solve it for $n = 2i$, $\forall i \in [0, \frac{N-1}{2}] \cap \mathbb{N}$, we will obtain the trajectory of the synaptic conductances.

4.4.1 Algorithm and results

The algorithm that we want to develop has as input an observable data of the synaptic conductances that we want to estimate. This allows as to compare the obtained estimations with the original conductances.

We consider that we have a time set $\{t_0, ..., t_N\}$ where the functions g_E and g_I are evaluated, giving the following two sets as inputs: $\{g_{E_0}, ..., g_{E_N}\}$ and $\{g_{I_0}, ..., g_{I_N}\}$.

To estimate the trajectories of g_E and g_I we have to have the trajectory of the variables V and w, so, the first step will be the computation of this trajectories. Assuming that the trajectory of the membrane

potential follow the Morris-Lecar equations, and defining the initial conditions $V(t_0) = V_0$ and $w(t_0) = w_0$, we can obtain the trajectories of V and w integrating the differential equation:

$$\begin{cases} C\dot{V} = I_{app} - \bar{g_{\mathrm{K}}} w(V - V_{\mathrm{K}}) - \bar{g_{Ca}} m_{\infty}(V)(V - V_{\mathrm{Ca}}) - g_L(V - V_L) - I_{syn} \\ \dot{w} = \phi(\frac{w_{\infty}(V) - w}{\tau_w(V)}) \end{cases}$$

where I_{syn} will be the original synaptic current defined by the knowing original trajectories of g_E and g_I.

For the integration of this system we will consider that time step integration is $\delta = \frac{t_{i+1} - t_i}{2}$, $\forall i \in [0, N-1] \cap \mathbb{N}$, and that the synaptic conductances are held constant for two integration steps:

$$g_{E\,n} = g_{E\,n+\delta}$$

$$g_{I\,n} = g_{I\,n+\delta}$$

for $\forall n \in [0, N]$, where $g_{E\,n+\delta} = g_E(t_n + \delta)$.

The solution of this integration will be the following two sets: $\{V_0, V_\delta, V_1, V_{1+\delta}, ..., V_N, V_{N+\delta}, V_{N+1}\}$ and $\{w_0, w_\delta, w_1, w_{1+\delta}, ..., w_N, w_{N+\delta}, w_{N+1}\}$.

After this computations we construct the system of equations and, solving it, we look for the estimation of the synaptic conductances that we will the following notation $\hat{g}_E$ and $\hat{g}_I$. So, $\forall n \in [0, N]$ we solve the system of equations:

$$\begin{cases} V_{n+\delta} = V_n + \frac{\delta}{C}\left[f_1(V_n, w_n) + \hat{g}_{E\,n}(V_n - VE) + \hat{g}_{I\,n}(V_n - VI)\right] \\ V_{n+1} = V_{n+\delta} + \frac{\delta}{C}\left[f_1(V_{n+\delta}, w_{n+\delta}) + \hat{g}_{E\,n}(V_{n+\delta} - VE) + \hat{g}_{I\,n}(V_{n+\delta} - VI)\right] \end{cases}$$

In this chapter, we have constructed this algorithm in order to find the estimation of the synaptic conductances $\hat{g}_E$ and $\hat{g}_I$. In order to have more general results, we have implemented this algorithm using different integration methods for the computation of the trajectory of V and w.

First of all we have used the Euler method to integrate numerically the Morris-Lecar equations. This means that given the input set $\{(g_{E\,n}, g_{I\,n})\}_{\forall n \in [0,N]}$, and the initial conditions $V(t_0) = V_0$ and $w(t_0) = w_0$, we compute the trajectory of V and w.

So, it's clear that if we try to solve the system of equations presented above in order to estimate the synaptic conductances $\hat{g}_E$ and $\hat{g}_I$, as we are integrating the system using the Euler method and recuperating the synaptic conductances also using the Euler equation, $\forall n \in [0, N] \cap \mathbb{N}$ we would expect to have that:

$$\hat{g}_{E\,n} = g_{E\,n}$$

$$\hat{g}_{I\,n} = g_{I\,n}$$

In Figure 36 it can be seen the estimated and original trajectories. As we have said, the trajectories coincide at each instant of time. We can compute the root square mean error between the estimated and the original trajectories, and we can see that the $RSMD(\hat{g}_E) = 6.86 \times 10^{-7}$ and $RSMD(\hat{g}_I) = 1.06 \times 10^{-6}$.

The obtained results are the expected ones because we have used the same integration method for the obtaining of the trajectory of V and for the reconstruction of the trajectory of the synaptic conductances from the voltage.

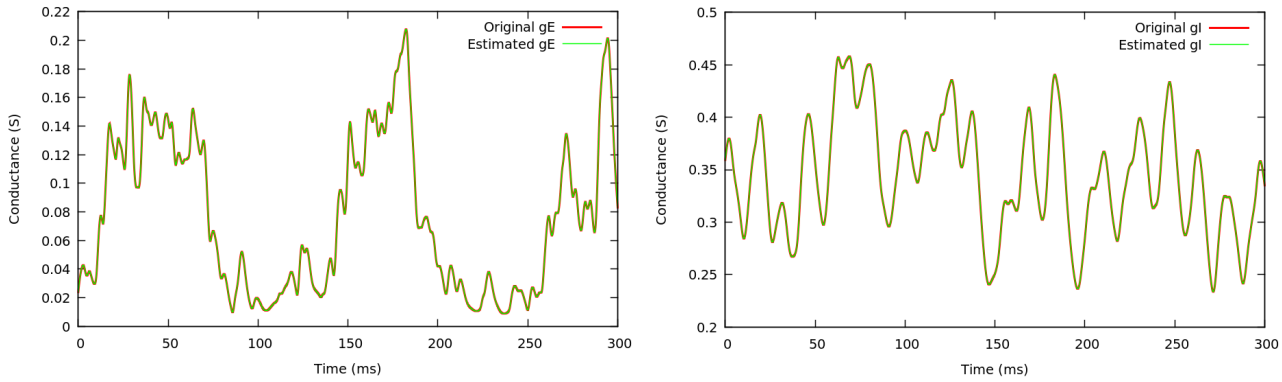

Figure 36: Comparison between the estimated and original synaptic conductances.

The following natural step is to try to do the same but using different methods for the integration of the membrane potential.

For the integration of the ODE we are going to use the Runge-Kutta 4th order method. Given a ordinary differential equation:

$$\begin{cases} \dot{y} = f(t, y) \\ y(t_0) = y_0 \end{cases}$$

Then, denoting with δ the constant integration step, the Runge-Kutta 4th order method for this problem is given by the following equation:

$$y_{n+1} = y_n + \frac{1}{6}\delta(k_1 + 2k_2 + 2k_3 + k_4)$$

where:

$$\begin{cases} k_1 = f(t_n, y_n) \\ k_2 = f(t_n + \frac{1}{2}\delta, y_n + \frac{1}{2}k_1\delta) \\ k_3 = f(t_n + \frac{1}{2}\delta, y_n + \frac{1}{2}k_2\delta) \\ k_4 = f(t_n + \delta, y_n + k_3\delta) \end{cases}$$

After computing the trajectory of V and w using the Runge-Kutta 4th order method, we find $\hat{g}_E$ and $\hat{g}_I$ as before. If, we compute the root square mean error of the estimations we have that $RSMD(\hat{g}_E) = 0.108$ and $RSMD(\hat{g}_I) = 0.037$. It is clear that the estimation is not as good as the obtained using the Euler integration method, but as we can see in Figure 37 this larger error seems to be caused by the points where the estimated function increase or decrease abruptly. At these points it seams that we have an asymptote. As we can see in Figure 38, the asymptotic points correspond to a maximum and minimum points of the membrane potential function V. This causes the asymptotic behaviour at the points where $|V_{n+1} - V_n| < \varepsilon$ with $\epsilon << 1$.

So, to have a better approximation of the synaptic conductances, we try to avoid the points where we can have this problem. So, we are going to save the trajectory of $\hat{g}_E$ and $\hat{g}_I$ where $|V_{n+1} - V_n| > 10^{-5}$.

In Figure 39 we can see that we have eliminated the problematic points when $t \in [50, 100]$, but in the spikes region we continue having the same problems.

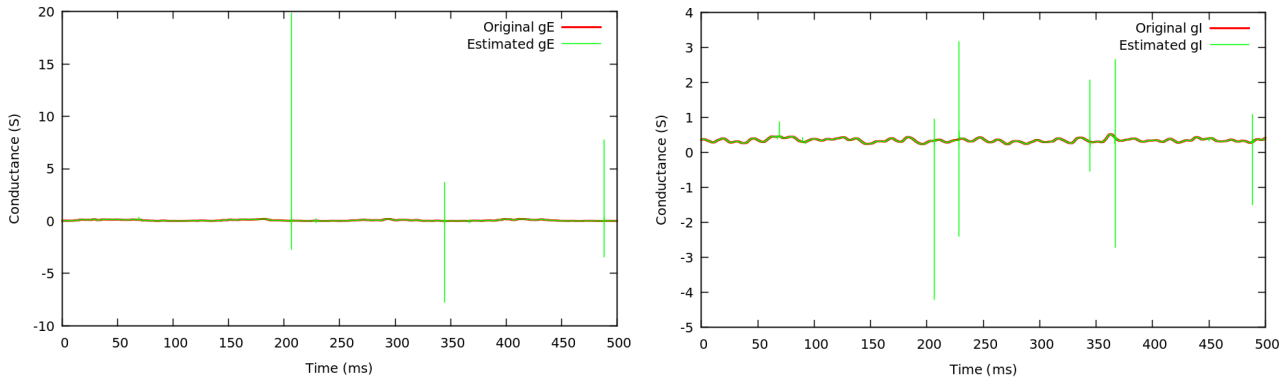

Figure 37: Comparison between the estimated and original synaptic conductances.

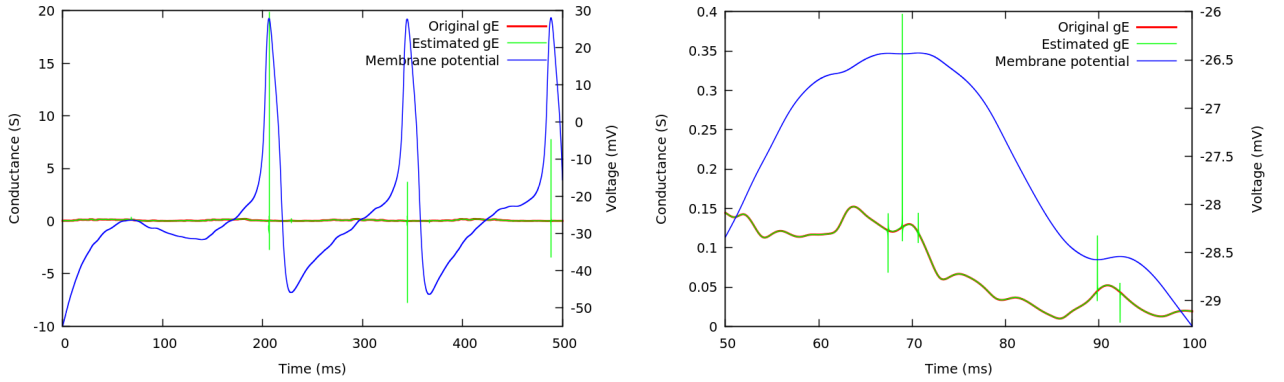

Figure 38: Comparison between the estimated and original synaptic conductances with the membrane potential trajectory.

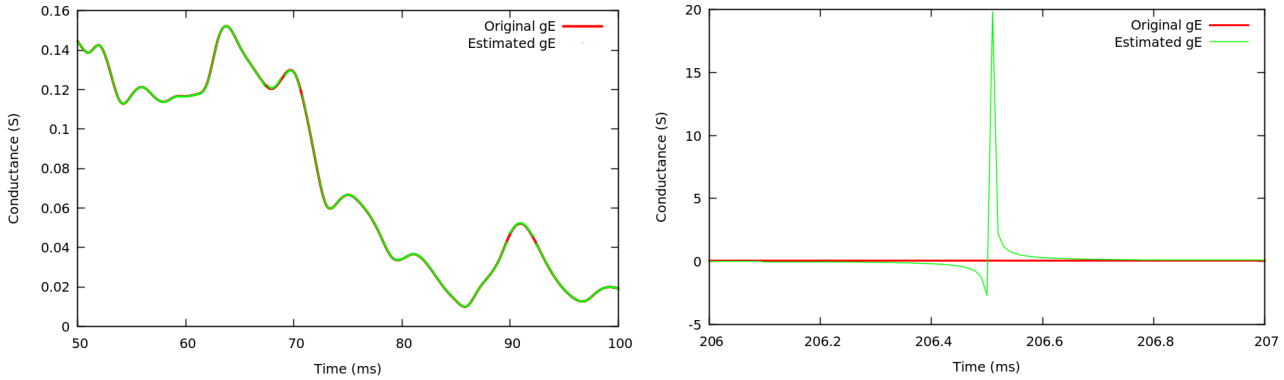

Figure 39: Trajectory of the estimated function $\hat{g}_E$ eliminating the problematic points.

In this last part we have shown theoretically that it is possible to extract conductances from single trances of the membrane potential recordings, under some conditions. First of all the membrane potential must be subthreshold. In this case that the equation that models V remains linear and the synaptic conductances can be estimated rigorously. If V contains spiking regimes then the estimation of g_E and g_I in this zones

have to be avoid because the underlying membrane equation is nonlinear.

To conclude, the previous method gives a better approximation estimation of the synaptic conductances than the control method presented at this project. However, the method presented by Claude Bédard and Alain Destexhe is not functional when the membrane potential contains actions potentials.

5. Discussion

In this project, we have presented two different methods for the estimation of synaptic conductances from an experimentally observable membrane potential of a neuron.

The main method is based on the use of control theory tools for the estimation of the synaptic current I_{syn} from a single trace of membrane potential recording. Notice that in Chapter 3 we have introduced some of the main obstacles that appear on the use of inverse methods. Knowing them we can conclude that the control method presented for the estimation of the synaptic current gives satisfactory results and it is functional because it avoids most of these problems.

First of all, to obtain a copy of the trajectory of I_{syn} we only need to record a single register of the membrane potential. Also, we have seen that the method gives an accurate estimation of the synaptic current in the spiking regimes where the underlying membrane equation is nonlinear. However, it is possible to estimate this synaptic parameter under some conditions.

This method is really dependent on the model that we are using as a connection between the observable membrane potential and the synaptic current. Further, this method is been developed for the utilization of conductance-based models, see Chapter 3.2. To solve this dependence in the neuronal model, we could use model' estimation methods from the observable membrane potential. There is a line of research called *genetic programming* that tries to do that.

For the extraction of the synaptic conductance from the estimated synaptic current we require an oversampling factor between the time course $\hat{I}_{syn}$ and the conductances to extract. During two integration steps we impose that the synaptic conductances remain constant. Even if we have an accurate estimation of the synaptic current, the estimated $\hat{I}_{syn}$ is not close enough to the original to have a good estimation of the synaptic conductances.

To improve the estimation of the synaptic current we could try to apply to the control variable u a more complex filter. In this project, we have used a simple linear filter and this can help to the generation of the small root mean square error between the original and estimated synaptic current. For example, a non-linear filter could reduce this error, and consecutively the method could give a more accurate estimation of the synaptic conductances g_E and g_I.

However, we have implemented an alternative way to extract the synaptic conductances from an experimental membrane potential in order to present a method that gives successful results.

With this alternative method, we can extract the synaptic conductances when we avoid the spiking regime. In these zones, the model that we are using becomes nonlinear and the method fails.

We have to note that these two methods are interesting because most of the existent methods for the estimation of the synaptic conductances can not extract the full-time course of them from a single trace of the membrane potential activity. For example, one can extract excitatory and inhibitory conductances from a membrane potential by building current-voltage relations with repeated trials. However, this approach requires repeated trials at different values of I_{app}.

An extension of this project could be the solution to the main problems that we have obtained during the estimation of the synaptic current using the control method. We have seen that this method gives

successful results for the estimation of the function I_{syn}, even in the non-linear zones. Therefore, if we use a more complex filter for u we could reduce the root mean square error obtained between the estimated and original synaptic current and obtain a better estimation of g_E and g_I even in the spiking regimes.

References

[1] Bédard, C., Béhuret, S., Deleuze, C., Bal, T., and Destexhe, A. Oversampling method to extract excitatory and inhibitory conductances from single-trial membrane potential recordings. *Journal of Neuroscience Methods 210*, 1 (2012), 3 – 14.

[2] Ermentrout, B., and Terman, D. *The Mathematical Foundations of Neuroscience*, vol. Vol. 35. 07 2010.

[3] Izhikevich, E. M. *Dynamical Systems in Neuroscience: The Geometry of Excitability and Bursting*, vol. Vol. 50. 01 2007.

[4] McLaughlin, D., Shapley, R., Shelley, M., and Wielaard, D. J. A neuronal network model of macaque primary visual cortex (V1): orientation selectivity and dynamics in the input layer 4Calpha. *Proceedings of the National Academy of Sciences of the United States of America 97*, 14 (July 2000), 8087–8092.

[5] Utkin, V. *Sliding Modes in Control and Optimization*. Springer-Verlag Berlin and Heidelberg GmbH Co. KG, 01 1992.

[6] Vich Llompart, C. *Inverse methods to estimate synaptic conductances with emphasis on non-smooth dynamical systems*. Doctoral programme of mathematics, Universitat de les Illes Balears, July 2016.